Supplement of

Trifluoroacetic acid enhances sulfuric acid–ammonia nucleation in the cold atmosphere: Molecular mechanism and atmospheric implications

Ling Liu et al.

Corresponding to: Xiuhui Zhang (zhangxiuhui@bit.edu.cn)

Section S1. Details about the method calculating single point energy.

Section S2. Details about the ACDC.

Section S3. Evidence for the consistency between theoretical predictions and existing experimental results.

Section S4. Details about the calculation of the proton-transfer parameter.

Section S5. Details about the kinetic stability of clusters.

Section S6. Concentrations of TFA in the upper troposphere.

Section S7. Scenarios under which the SA–NH_3–TFA nucleation mechanism is atmospheric relevant.

Section S8. Influence of water vapor and atmospheric pressure on the particle formation rates of SA-NH_3-TFA nucleation system.

Table S1. Cartesian coordinates of the $(SA)_x \cdot (NH_3)_y \cdot (TFA)_z$ clusters ($1 \le y \le x + z \le 3$, $z = 1, 2, 3$) in the present study at the M06-2X/6-311++G(3df,3pd) level of theory.

Table S2. Atoms in molecules (AIM) topological parameters for the stable clusters obtained at the M06-2X/6-311++G(3df,3pd) level.

Table S3. Proton-transfer parameter (ρ_{PT}, Å) and the total number of proton transfers (n) for $(SA)_x \cdot (NH_3)_y \cdot (TFA)_z$ ($0 \le y \le x+z \le 3$, $z = 1, 2, 3$). r_{OH} and $r_{H\cdots N}$ are the bond distances between the O and H atoms and that between the H and N atoms, respectively.

Table S4. Gibbs free formation energies (ΔG, kcal mol^{-1}) of the studied clusters at different temperatures at the RI-CC2/aug-cc-pV(T + d)Z//M06-2X/6-311++G(3df,3pd) level of theory.

Table S5. Gibbs free formation energies (ΔG, kcal mol^{-1}) with a scaling factor of 0.97 for Zero-Point Energies of the studied clusters at different temperatures at the RI-CC2/aug-cc-pV(T + d)Z//M06-2X/6-311++G(3df,3pd) level of theory. p = 1 atm.

Table S6. Collision coefficients (β, $cm^3\ s^{-1}$) for each cluster in the present study.

Table S7. Total evaporation coefficients ($\Sigma\gamma$, s^{-1}) of each cluster in the present study.

Table S8. Ratios ($\beta C/\Sigma\gamma$) between monomer molecule collisions and evaporation coefficients of each cluster involving TFA in the present study. [SA] = 7.0×10^5 molecules cm^{-3}, [NH_3] = 1.0×10^{10} molecules cm^{-3}, [TFA] = 1.0×10^6 molecules cm^{-3}.

Table S9. Contributions of different formation pathways of $(SA)_3 \cdot (NH_3)_3$ and $(SA)_2 \cdot (NH_3)_3 \cdot (TFA)_1$ clusters to the main cluster formation pathway and the thermodynamic barriers (kcal mol^{-1}) of main pathway involving TFA [from $(SA)_1 \cdot (NH_3)_1$ cluster to

$(SA)_1 \cdot (NH_3)_1 \cdot (TFA)_1$ cluster] at different nucleation precursor concentrations and different temperatures (T, 240 K, 230 K, and 220 K). CS = 2.0×10^{-2} s^{-1}.

Table S10. Relative hydrate distributions of the clusters at varying relative humidities (RHs) at different temperatures.

Table S11. Ratios ($\beta C/\Sigma\gamma$) between monomer molecule collisions and evaporation coefficients of $(SA)_1 \cdot (NH_3)_{1\text{-}2} \cdot (TFA)_1$ cluster at different relative humidities (RHs) and different temperatures. C = 1.0×10^{6} molecules cm^{-3}.

Table S12. Gibbs free formation energies (ΔG, kcal mol^{-1}) of the studied clusters at different pressures at the RI-CC2/aug-cc-pV(T + d)Z//M06-2X/6-311++G(3df,3pd) level of theory.

Table S13. Particle formation rates (J, cm^{-3} s^{-1}) of the studied clusters at different pressures at 240 K. [SA] = 5.0×10^{6} molecules cm^{-3}, [NH_3] = 1.0×10^{11} molecules cm^{-3}, [TFA] = 1.0×10^{6}–1.0×10^{8} molecules cm^{-3}.

Fig. S1. The electrostatic potential (ESP, kcal mol^{-1}) mapped molecular van der Walls (vdW) surfaces of the SA, NH_3, and TFA molecules at the M06-2X/6-311++G(3df,3pd) level of theory. Surface local minima and maxima of the ESP are shown as yellow and cyan dots, respectively. The C, H, N, O, S, and F atoms are shown as cyan, white, blue, red, yellow, and pink spheres, respectively.

Fig. S2. Particle formation rates (J, cm^{-3} s^{-1}) at different [TFA] and 240 K. [SA] = 5.0×10^{6} molecules cm^{-3}, [NH_3] = 1.0×10^{11} molecules cm^{-3}. The black and red lines correspond to the simulated J based on the calculated Gibbs free energy of cluster formation without scaling factor and with Zero Point Energy (ZPE) scaling factor of 0.97.

Fig. S3. Particle formation rates (J, cm^{-3} s^{-1}) at different temperatures as a function of (a) [SA], (c) [NH_3], and (e) [TFA]. Enhancement on particle formation rate by TFA (R_J, $R_J = J_{SA\text{-}NH3\text{-}TFA}/J_{SA\text{-}NH3}$) at different temperatures as a function of (b) [SA], (d) [NH_3], and (f) [TFA]. Black, red, and blue lines are corresponding to the J at 240 K, 230 K, and 220 K, respectively. CS = 2.0×10^{-3} s^{-1}.

Fig. S4. Concentrations (molecules cm^{-3}) at different temperatures as a function of (a) [SA], (c) [NH_3], and (e) [TFA]. Enhancement by TFA on concentrations of clusters (R_C, $R_C = C_{SA\text{-}NH3\text{-}TFA}/C_{SA\text{-}NH3}$) at different temperatures as a function of (b) [SA], (d) [NH_3], and (f) [TFA]. CS = 2.0×10^{-3} s^{-1}. (a) and (b): [NH_3] = 1.0×10^{10} molecules cm^{-3}, [TFA] = 1.0×10^{7} molecules cm^{-3}. (c) and (d): [SA] = 7.0×10^{5} molecules cm^{-3}, [TFA] = 1.0×10^{7} molecules cm^{-3}. (e) and (f): [SA] = 7.0×10^{5} molecules cm^{-3}, [NH_3] = 1.0×10^{11} molecules cm^{-3}.

Fig. S5. Main cluster formation pathways of SA-NH_3-TFA clusters at [SA] = 7×10^5 molecules cm^{-3}, [NH_3] = 1×10^{11} molecules cm^{-3}, and [TFA] = 1×10^8 molecules cm^{-3}. Blue arrows show the pathways involving TFA and grey arrows show the pathways without TFA. The pathways covered by the light blue shadow are only present at 240 K and 230 K, but not present at 220 K. The pathways covered by the light blue shadow are only present at 240 K and 230 K, but not present at 220 K. The pathways without light blue shadow are the common pathways at different temperatures (240 K, 230 K, and 240 K). The values of contribution (percentage) shown in black, red, and blue are corresponding to the contributions to the formation of the relevant larger clusters at 240 K, 230 K, and 220 K.

Fig. S6. Comparison of particle formation rates (J, cm^{-3} s^{-1}) between SA–NH_3–TFA and SA–NH_3–NA under selected upper tropospheric sensitivity conditions as a function of [NH_3] at 220 K. Blue and red lines show the J for SA–NH_3–TFA at the concentration of TFA at 1.0×10^8 molecules cm^{-3} and 1.0×10^5 molecules cm^{-3}, respectively. Black line shows the J for SA–NH_3–NA. [SA] = 1.0×10^5 molecules cm^{-3}, [NA] = 1.5×10^9 molecules cm^{-3}.

Section S1. Details about the method calculating single point energy.

Although DLPNO-CCSD(T) [6–8] yields more accurate energy values than RI-CC2, the simulated SA dimer concentrations and the particle formation rate of SA-dimethylamine system calculated via the combination of Atmospheric Cluster Dynamics Code (ACDC) and DLPNO-CCSD(T)/aug-cc-pVTZ//M06-2X/6-311++G(3df,3pd) are both approximately one order of magnitude lower than the currently available field-measurements (e.g., in Shanghai) [2]. In contrast, the simulated SA dimer concentrations obtained from the combination of ACDC and RI-CC2/aug-cc-pV(T+d)Z are in good agreement with the field observations in Shanghai [2]. Furthermore, the particle formation rates of the SA-DMA system predicted by ACDC coupled with RI-CC2/aug-cc-pV(T+d)Z//M06-2X/6-311++G(3df,3pd) correlate well with both field measurements in Shanghai and the experimental results from the CLOUD chamber [2]. These favorable agreements may be attributed to a random cancellation of errors. Accordingly, we adopted the RI-CC2/aug-cc-pV(T+d)Z//M06-2X/6-311++G(3df,3pd) level of theory to simulate the SA-NH_3-TFA nucleation processes.

Section S2. Details about the ACDC.

The ACDC is a widely used study the first steps of atmospheric new particle by examining the formation of atmospheric molecular clusters [9–11]. It models the cluster kinetics by explicit solution of the birth–death equations, enabling us to quantitatively describe the dynamic evolution of clusters formation from molecular precursors. In our study, ACDC is employed to quantitatively model the dynamic evolution of SA–NH_3–TFA clusters under atmospheric conditions. It takes the cluster formation Gibbs free energies (ΔG) from quantum chemical calculations as key input to determine evaporation coefficients, and then computes collision coefficients based on kinetic gas theory. ACDC can describe the formation, collision, evaporation, growth, and loss of molecular clusters, which allows us to obtain the kinetic characteristics of nucleation that cannot be provided by quantum chemistry alone. This makes ACDC indispensable for evaluating the feasibility of the nucleation mechanism and comparing with field and chamber observations.

The primary outputs of the ACDC code include:

(1) Collision coefficients and evaporation coefficients for each cluster growth step.

(2) Steady-state or time-dependent number concentrations of all simulated molecular clusters.

(3) Cluster formation rates (J) under different temperature and precursor concentration conditions.

(4) Dominant cluster formation pathways and flux distributions between clusters.

Section S3. Evidence for the consistency between theoretical predictions and existing experimental results.

Atmospheric nucleation involves elusive molecular clusters with small size and trace concentrations, which are challenging to detect and characterize experimentally, especially under upper tropospheric conditions (high altitude, low temperature, and trace precursor concentrations). Consequently, no direct experimental evidence to support the proposed mechanism. In this case, theoretical calculations can serve as an indispensable preliminary approach to unravel molecular-scale nucleation mechanisms. The rationality of the proposed mechanism can be validated through the following existing experimental evidence, rather than relying solely on theoretical deductions:

(1) Experimental verification of our theoretical method

The reliability of the combined approach of quantum chemical calculations (RI-CC2//M06-2X) and Atmospheric Cluster Dynamics Code (ACDC) simulations adopted in this study has been directly verified by experimental data in analogous nucleation systems. For example:

a) The $(SA)_1 \cdot (DMA)_{1\text{-}2} \cdot (TFA)_1$ clusters and their concentrations, previously predicted via quantum chemical calculations coupled with ACDC simulations, are in accordance with field measurements using CI-APi-TOF with tofTools software in Shanghai, China [1]. This cannot only verify the reliability of our theoretical method, but also confirm TFA's nucleation ability in the atmosphere.

b) The simulated particle formation rates (J) of the SA-NH_3-HNO_3 nucleation system were compared with published CLOUD chamber data. At the same NH_3 concentrations, the J values of the SA-NH_3-HNO_3 system fall within the same order of magnitude as those from CLOUD (Fig. 4a), confirming that our theoretical method can accurately reflect the kinetic characteristics of actual atmospheric nucleation.

c) For the sulfuric acid-dimethylamine (SA-DMA) system, not only are the simulated SA dimer concentrations in good agreement with field measured results in Shanghai, but also the J values are consistent with both the field-measured results in Shanghai and the experimental results of the CLOUD chamber [2–5], further verifying the reliability of our theoretical method.

We now state the above experimental verifications in Section S2 of the revised Supplementary Materials.

(2) Cross-system experimental analogy for the nucleation mechanism

We compared our predicted particle formation rates with the CLOUD chamber experimental data for the SA–NH_3–HNO_3 system. The results reveal that the SA–NH_3–TFA mechanism achieves comparable formation rates to those of the SA–NH_3–HNO_3 mechanism under realistic upper tropospheric [NH_3] conditions, demonstrating that our newly proposed SA–NH_3–TFA mechanism is of comparable significance to the well-established SA–NH_3–HNO_3 mechanism. We now state the above details in Section S2 of the revised Supplementary Materials.

In summary, although direct experimental data for the SA-NH_3-TFA system are not provided in this study, the rationality of the proposed mechanism is fully supported by the above experimental results. Future targeted experiments can be conducted based on the theoretical predictions of this study to obtain further direct experimental evidence.

Section S4. Details about the calculation of the proton-transfer parameter.

The proton-transfer parameter (ρ_{PT}) can be used to assess the degree of ionization based on the interatomic distances. It can be formulated as

$$\rho_{PT} = (r_{OH} - r_{OH}^0) - (r_{H\cdots N} - r_{H\cdots N}^0)$$

where r_{OH} and r_{OH}^0 are the O-H distances in TFA or SA within the clusters and those in monomer molecule, respectively. The $r_{H\cdots N}$ and $r_{H\cdots N}^0$ are the hydrogen bond distances in TFA/SA-NH_3-based clusters and the H-N distance in fully protonated NH_3 (NH_4^+), respectively. The ρ_{PT} is negative for hydrogen-bonded cluster while positive for fully proton-transferred cluster.

Section S5. Details about the kinetic stability of clusters.

The collision rate coefficients $\beta_{i,j}$ between clusters i and j were calculated using the hard-sphere collision model [12], as follows:

$$\beta_{i,j} = \pi\left(r_i + r_j\right)^2 \sqrt{\frac{8k_BT}{\pi\mu}}, \qquad \text{(S1)}$$

where r_i denotes the radius of cluster i given by Multiwfn 3.3.8 program [13], k_B is the Boltzmann constant, T is the temperature, and $\mu = m_i m_j/(m_i+m_j)$ is the reduced mass.

Evaporation coefficients, $\gamma_{(i+j)\rightarrow i}$, were determined from the corresponding collision coefficients and ΔG of clusters [14]:

$$\gamma_{(i+j)\rightarrow i} = \beta_{i,j}\frac{p_{ref}}{k_BT} exp\left(\frac{\Delta G_{i+j}-\Delta G_i-\Delta G_j}{k_BT}\right), \qquad \text{(S2)}$$

where p_{ref} is the reference pressure (1 atm herein) at which the Gibbs free energies of formation were calculated, and ΔG_i denotes the formation Gibbs free energy of cluster i from constituent monomers.

At a certain monomer concentration (C), the $\beta \cdot C$ of each cluster decreases with the decreasing of temperature (Table S5). The total $\sum\gamma$ of each cluster also decreases with the decreasing of temperature (Table S6). The $\beta \cdot C/\sum\gamma$ of other $(SA)_x \cdot (NH_3)_y \cdot (TFA)_1$ ($0 \le x \le 2$, $1 \le y \le 3$, $y \le x+1$) clusters based on different nucleation monomer collisions at different temperatures are shown in Table S8, and they are all in negative correlation with temperature. The $\beta \cdot C/\sum\gamma$ of $(SA)_2 \cdot (NH_3)_3 \cdot (TFA)_1$ cluster is greater than one at 240 K, 230 K, and 220 K, which indicates that this cluster has the potential to grow into larger clusters throughout the upper troposphere. Besides $(SA)_2 \cdot (NH_3)_3 \cdot (TFA)_1$ cluster, the $(SA)_3 \cdot (NH_3)_3$ cluster, whose $\beta \cdot C/\sum\gamma$ is greater than one at the studied temperatures, also has the ability to grow into larger clusters. The boundary of the ACDC simulation is the smallest clusters that can be stable enough to grow outside of the simulated system[14]. Therefore, $(SA)_3 \cdot (NH_3)_3 \cdot (TFA)_1$ and $(SA)_4 \cdot (NH_3)_3$ clusters were set as the boundary of the following ACDC simulation.

Section S6. Concentrations of TFA in the upper troposphere.

At present, there are no direct observational constraints on TFA concentrations in the upper troposphere, so we cannot provide a specific measured value for this region. The TFA concentrations used in this study are referenced to field measurements in the lower troposphere, which range from 1.0×10^6 to 1.0×10^8 molecules cm^{-3} [15,16]. These concentrations should therefore be regarded as a sensitivity-analysis range, rather than an observationally constrained one.

Nevertheless, two lines of indirect evidence suggest that the presence of TFA in the upper troposphere is plausible. First, perfluorocarboxylic acids, such as perfluorooctanoic acid (PFOA) and perfluorononanoic acid (PFNA), have been detected in the upper troposphere and are linked to convective transport from surface anthropogenic sources [17]. Although this does not imply identical transport efficiency for TFA, it supports the general possibility that persistent TFA, as a representative of perfluorocarboxylic acids, can be transported to high altitudes. Second, hydrofluorocarbons (HFCs), which are important precursors of TFA, have been detected in the upper troposphere [18], implying that oxidative degradation of these precursors could contribute to TFA formation aloft. Hence, TFA can exist in the upper atmosphere.

However, these arguments support only the plausibility of TFA being present in the upper troposphere/near-tropopause region. They do not quantitatively constrain its concentration there. Accordingly, we do not claim that TFA concentration is generally comparable sulfuric acid concentration in this region. Rather, we selected a broad sensitivity range to test whether TFA could influence SA–NH_3 nucleation under upper-atmospheric scenarios, including cases in which its abundance approaches the order of magnitude of sulfuric acid under some conditions. Direct measurements of TFA in the upper troposphere/near-tropopause region are still needed to assess the real atmospheric significance of this mechanism.

Section S7. Scenarios under which the SA–NH_3–TFA nucleation mechanism is atmospheric relevant.

Considering the atmospheric transport of TFA in the lower troposphere cannot be assumed to be loss-free, we clarify the possible scenarios that enable TFA to be effectively transported to the upper troposphere and retain sufficient concentrations to participate in nucleation processes as follows:

(1) Rapid deep convective uplift, which reduces the time available for multiphase processing and subsequent removal in the lower troposphere.

(2) Abundant TFA precursor species aloft, such that the in-situ production can contribute to the TFA concentrations and upper-tropospheric TFA concentrations are not solely dependent on near-surface transport.

Section S8. Influence of water vapor and atmospheric pressure on the particle formation rates of SA-NH_3-TFA nucleation system.

(1) Although water vapor is ubiquitous in the atmosphere and may play a role in nucleation, the introduction of hydrated clusters requires extensive additional quantum chemical calculations that are time-consuming in the current computational workflow. We studied the influence of different relative humidities (RHs) on the population and stability of the $(SA)_1 \cdot (TFA)_1$, $(NH_3)_1 \cdot (TFA)_1$, $(SA)_1 \cdot (NH_3)_1 \cdot (TFA)_1$ and $(SA)_1 \cdot (NH_3)_2 \cdot (TFA)_1$ clusters with fewer molecules involved in the initial nucleation process. Although the relative hydration distribution of these clusters (which bind abundant water molecules, Table S10) increases with rising RH, their effective ratios of monomer molecule collisions to evaporation coefficients, calculated as a weighted average over the hydrate distribution, show negligible sensitivity to RH (Table S11). Specifically, these parameters vary by less than one order of magnitude.

(2) As the atmospheric pressure decreases with the increasing of altitude, the influence of pressure variation from 0.2 atm to 1.0 atm across the troposphere [19] on particle formation was also studied. Taking 240 K as an example, as shown in Table S11, the ΔG of the studied clusters increases with the decreasing pressure, with the variation of up to 3.8 kcal/mol. The influence of pressure variation on the particle formation rates is almost negligible (Table S12). Hence, we primarily investigated the particle formation rates and corresponding formation pathways at 1.0 atm.

Table S1. Cartesian coordinates of the $(SA)_x \cdot (NH_3)_y \cdot (TFA)_z$ clusters ($1 \leq y \leq x + z \leq 3$, $z \geq 1$) in the present study at the M06-2X/6-311++G(3df,3pd) level of theory.

$(NH_3)_1 \cdot (TFA)_1$

Atoms	X	Y	Z
C	0.298745	0.208042	-0.004770
O	0.758945	1.314441	-0.004131
O	0.946188	-0.924740	-0.005900
H	1.946670	-0.728163	-0.003800
C	-1.228491	-0.031689	0.000062
F	-1.588673	-0.700578	1.093191
F	-1.592574	-0.748284	-1.060330
F	-1.885581	1.113159	-0.023995
N	3.470133	-0.105307	0.002763
H	3.222051	0.879954	0.012430
H	4.038730	-0.276350	-0.817691
H	4.040484	-0.292701	0.818429

$(NH_3)_1 \cdot (TFA)_2$

Atoms	X	Y	Z
C	-2.249005	0.241741	-0.000257
O	-1.144912	-0.250304	-0.002574
O	-2.560343	1.485192	0.001620
H	-1.692633	2.118568	0.000790
C	-3.502394	-0.666436	0.000423
F	-4.244315	-0.425960	-1.076253
F	-4.243034	-0.426525	1.078070
F	-3.164067	-1.942638	-0.000119
C	2.230174	0.079468	-0.000416
O	1.945598	1.243914	0.000761
O	1.424007	-0.943207	-0.002385
H	0.481341	-0.654545	-0.002657
C	3.701063	-0.395410	0.000269
F	3.944545	-1.132462	-1.078075
F	3.942390	-1.136155	1.076538
F	4.525739	0.634513	0.002897
N	-0.495799	2.994650	-0.000415
H	0.339560	2.408109	-0.000060
H	-0.451146	3.594602	0.815479
H	-0.451675	3.592821	-0.817651

$(NH_3)_2 \cdot (TFA)_2$

Atoms	X	Y	Z
C	2.183110	-0.712264	-0.281731
O	1.293243	-0.075078	-0.873116
O	2.171379	-1.896372	0.075834
H	0.645602	-2.250659	0.026880
C	3.466487	0.100793	0.041062
F	4.258000	-0.494043	0.914079
F	3.131463	1.302873	0.552474
F	4.166764	0.332627	-1.068228
C	-2.183109	0.712263	0.281735
O	-1.293239	0.075074	0.873112
O	-2.171378	1.896372	-0.075826
H	-0.645604	2.250657	-0.026887
C	-3.466488	-0.100792	-0.041056
F	-4.258006	0.494049	-0.914066
F	-4.166758	-0.332634	1.068235
F	-3.131466	-1.302869	-0.552477
N	-0.428338	-2.287173	-0.003850
H	-0.800279	-3.085752	0.499052
H	-0.725654	-2.332860	-0.974163
H	-0.812524	-1.384344	0.398946
N	0.428337	2.287173	0.003828
H	0.812521	1.384337	-0.398957
H	0.725668	2.332881	0.974136
H	0.800270	3.085743	-0.499095

$(NH_3)_1 \cdot (TFA)_3$

Atoms	X	Y	Z
C	0.019706	1.600527	0.914334
O	-1.096699	1.276137	1.349230
O	1.116491	1.283111	1.403743
H	0.019422	-0.371838	2.397737
C	0.049955	2.493831	-0.351908
F	1.123870	2.236030	-1.091696
F	0.085994	3.776090	-0.001811
F	-1.028078	2.298555	-1.102925
C	3.214880	-0.656187	0.116152
O	2.313361	-1.407548	0.409803
O	3.268298	0.621316	0.258425
H	2.410423	0.985697	0.675791
C	4.527375	-1.218307	-0.478611

F	5.480357	-1.174386	0.450079
F	4.925409	-0.504459	-1.520524
F	4.370286	-2.473547	-0.857773
C	-3.256998	-0.642545	0.149346
O	-2.415419	-1.413699	0.549715
O	-3.231820	0.643950	0.158069
H	-2.373427	0.998206	0.581519
C	-4.571509	-1.175778	-0.467467
F	-4.681293	-0.776234	-1.728834
F	-5.614015	-0.711905	0.212085
F	-4.602556	-2.495289	-0.438066
N	-0.010422	-1.278899	1.924315
H	0.827042	-1.319525	1.308033
H	-0.891453	-1.303259	1.369944
H	0.007028	-2.046075	2.588984

$(NH_3)_2 \cdot (TFA)_3$

Atoms	X	Y	Z
C	-1.849293	-1.678455	0.507319
O	-1.657496	-1.582233	1.691792
O	-1.004166	-1.919092	-0.436530
H	0.011819	-1.874325	-0.114772
C	-3.274307	-1.520378	-0.071060
F	-3.693024	-2.666450	-0.599149
F	-3.265268	-0.605530	-1.053255
F	-4.136834	-1.135200	0.843882
C	-0.120608	1.956573	0.698595
O	-0.485508	0.879184	0.184917
O	0.405758	2.133846	1.799856
H	0.633302	0.685203	2.380781
C	-0.401815	3.229914	-0.143588
F	-0.337388	2.952658	-1.458785
F	0.451085	4.207145	0.101329
F	-1.633203	3.675163	0.102118
C	2.106225	-1.248320	-0.643034
O	1.353611	-1.718145	0.251781
O	1.844361	-0.959956	-1.803234
H	0.331286	-0.410082	-2.281687
C	3.561820	-1.033510	-0.153131
F	3.556402	-0.467393	1.064143
F	4.257305	-0.254155	-0.959479
F	4.192739	-2.200776	-0.047207
N	0.723436	-0.355690	2.630097
H	-0.197927	-0.797647	2.499068

H	1.067132	-0.492739	3.574017
H	1.338490	-0.811440	1.944186
N	-0.571775	0.122226	-2.314831
H	-0.653098	0.565530	-1.345958
H	-1.348657	-0.518556	-2.448206
H	-0.554933	0.835385	-3.035937

$(NH_3)_3 \cdot (TFA)_3$

Atoms	X	Y	Z
C	1.586381	-1.958739	-0.050474
O	1.187084	-2.286873	-1.198391
O	1.222801	-2.416602	1.044705
H	-0.436553	-4.548210	0.293556
C	2.720028	-0.900451	-0.022155
F	3.911896	-1.514651	-0.102278
F	2.709847	-0.182422	1.105196
F	2.641106	-0.047187	-1.058366
C	0.348345	1.612818	0.704908
O	0.080644	0.527058	0.125828
O	0.360567	1.849864	1.919041
H	0.001162	0.345400	2.553001
C	0.729612	2.815120	-0.200274
F	2.000171	3.180899	-0.001298
F	-0.050165	3.872761	0.035518
F	0.605611	2.513417	-1.513885
C	-2.309845	-1.108238	-0.160392
O	-2.122283	-1.722187	0.922786
O	-2.126380	-1.524985	-1.315355
H	-0.985301	-0.537766	-2.458403
C	-2.905553	0.316777	-0.023158
F	-4.246421	0.251987	-0.081145
F	-2.502177	1.122469	-1.018581
F	-2.580488	0.897833	1.137432
N	-0.031069	-0.143224	-2.435946
H	0.057118	0.336672	-1.492280
H	0.152147	0.503607	-3.200800
H	0.641761	-0.926193	-2.401211
N	-0.863687	-3.814902	-0.271997
H	-0.100374	-3.288221	-0.780752
H	-1.349074	-3.100467	0.338489
H	-1.542748	-4.191975	-0.932946
N	-0.219619	-0.678711	2.701011
H	-0.303873	-0.909106	3.690005
H	0.522100	-1.247954	2.248601

H	-1.093435	-0.907816	2.188300

$(SA)_1 \cdot (NH_3)_1 \cdot (TFA)_1$

Atoms	X	Y	Z
S	2.560118	-0.419195	0.016345
O	1.525786	-0.037785	0.988776
O	3.580932	-1.284437	0.499122
O	3.022421	0.778640	-0.680741
O	1.730933	-1.243041	-1.071972
H	2.061637	1.921877	-0.330408
H	2.193658	-2.070389	-1.246643
C	-1.534059	0.194203	0.171269
O	-1.140983	1.293966	-0.144966
O	-0.873951	-0.765461	0.714434
H	0.113005	-0.521138	0.838003
C	-3.009752	-0.201429	-0.069018
F	-3.579688	-0.565148	1.074428
F	-3.075647	-1.223852	-0.914168
F	-3.692715	0.808804	-0.575978
N	1.304124	2.577572	0.073002
H	1.277252	3.476287	-0.396594
H	1.508351	2.700957	1.061014
H	0.389545	2.086582	-0.007181

$(SA)_1 \cdot (NH_3)_2 \cdot (TFA)_1$

Atoms	X	Y	Z
S	-2.529226	-0.143412	0.255386
O	-2.111671	-0.023170	-1.124761
O	-2.369551	1.074649	1.028712
O	-1.977957	-1.316446	0.917342
O	-4.097420	-0.394820	0.147088
H	-0.806412	-1.939555	-0.137485
H	-4.466144	-0.451771	1.036895
C	1.830010	0.718808	-0.269701
O	1.851500	1.872658	0.160404
O	1.058444	0.228799	-1.123357
H	-0.892302	3.361986	-0.956698
C	2.894857	-0.262854	0.288843
F	3.928877	-0.347616	-0.549444
F	2.377523	-1.500151	0.400607
F	3.352241	0.088651	1.475836

N	-0.643096	2.449067	-0.593965
H	0.367091	2.405453	-0.267755
H	-0.744185	1.724980	-1.311730
H	-1.291963	2.154847	0.164364
N	-0.186875	-2.056128	-0.973875
H	0.418677	-1.172663	-1.045461
H	-0.798616	-2.087241	-1.785088
H	0.387547	-2.889053	-0.909603

$(SA)_1 \cdot (NH_3)_1 \cdot (TFA)_2$

Atoms	X	Y	Z
S	3.006250	0.142868	-0.290733
O	2.488784	-1.218132	-0.167960
O	3.099039	0.806831	0.990103
O	2.343025	0.894651	-1.337327
O	4.513550	0.014695	-0.741303
H	0.864174	1.446486	-1.251530
H	4.553946	-0.269633	-1.663156
C	-0.614046	-1.945196	0.028327
O	0.103425	-1.633132	-1.001797
O	-0.240059	-2.234384	1.136106
H	1.069620	-1.303982	1.987578
C	-2.119091	-1.900607	-0.317083
F	-2.430082	-0.707663	-0.824715
F	-2.857689	-2.104366	0.756041
F	-2.416899	-2.824315	-1.222941
C	-0.617962	1.456820	-0.069222
O	-0.067450	1.819755	-1.178534
O	-0.155604	0.736576	0.780960
H	1.072514	-1.526625	-0.736363
C	-2.005687	2.110296	0.123218
F	-2.689468	1.479424	1.063488
F	-2.711899	2.110280	-0.994193
F	-1.833260	3.374772	0.510391
N	1.397532	-0.521732	2.580960
H	0.589356	0.084190	2.716243
H	2.123990	0.022236	2.041362
H	1.760375	-0.862377	3.464818

$(SA)_1 \cdot (NH_3)_2 \cdot (TFA)_2$

Atoms	X	Y	Z

S	-3.252509	-0.111321	-0.009373
O	-2.892513	-0.929505	1.136068
O	-4.612811	-0.116205	-0.400388
O	-2.312523	-0.408120	-1.136554
O	-2.918371	1.382024	0.375612
H	-1.140075	-1.222190	-0.746912
H	0.148897	-0.766369	2.088660
C	0.883248	1.205574	0.888501
O	1.255540	0.236818	1.556212
O	-0.277097	1.572760	0.619965
H	-1.996214	1.431591	0.710929
C	2.000181	2.110373	0.300836
F	2.167942	3.178945	1.080071
F	1.652479	2.560106	-0.916553
F	3.157102	1.490226	0.188923
C	0.793013	-1.252788	-0.875210
O	-0.314171	-1.755987	-0.424920
O	0.931750	-0.299873	-1.595758
H	-0.137655	1.394438	-2.522550
C	2.014001	-2.077041	-0.405988
F	3.117634	-1.366710	-0.444389
F	2.155633	-3.132646	-1.207204
F	1.840300	-2.538062	0.835903
N	-0.574604	-1.507744	2.354372
H	-0.256456	-2.395957	1.974493
H	-1.490447	-1.264685	1.898014
H	-0.681444	-1.572217	3.361142
N	-0.945332	1.740031	-2.006181
H	-1.395908	2.520521	-2.471208
H	-0.607728	1.993541	-1.054154
H	-1.604156	0.937721	-1.847270

$(SA)_1 \cdot (NH_3)_3 \cdot (TFA)_2$

Atoms	X	Y	Z
S	2.907734	-1.368649	0.174708
O	1.574861	-1.770443	0.592719
O	3.986848	-2.217792	0.535233
O	3.194944	0.018143	0.888921
O	2.881402	-1.030400	-1.276216
H	2.365342	0.580466	0.936125
H	1.187763	-1.017899	-1.798725
C	0.459886	1.844083	0.017234
O	1.078473	1.521771	1.044352
O	0.858028	1.813292	-1.162768

H	2.434972	1.767054	-1.334149
C	-0.948503	2.452870	0.234821
F	-1.774528	2.188166	-0.765734
F	-0.821648	3.782741	0.317368
F	-1.504534	2.034634	1.367243
C	-2.185817	-0.953382	0.556741
O	-1.129823	-0.455227	0.103636
O	-2.471762	-1.167000	1.732425
H	-0.994148	-0.853019	2.440867
C	-3.258997	-1.300045	-0.508550
F	-4.015642	-0.232727	-0.756981
F	-4.048860	-2.293125	-0.139504
F	-2.678515	-1.652986	-1.670110
N	3.469164	1.519548	-1.467348
H	3.447387	0.460363	-1.526758
H	3.996144	1.766485	-0.633756
H	3.866554	1.957933	-2.290192
N	0.024529	-0.616522	2.590417
H	0.167845	0.362944	2.314010
H	0.592415	-1.170197	1.916589
H	0.328737	-0.777441	3.544062
N	0.204508	-0.817392	-2.069749
H	-0.403470	-0.754186	-1.178567
H	-0.159366	-1.527958	-2.695394
H	0.169029	0.104162	-2.501114

$(SA)_2 \cdot (NH_3)_1 \cdot (TFA)_1$

Atoms	X	Y	Z
S	3.111663	-1.458927	-0.264933
O	1.729343	-1.551105	0.143480
O	3.902265	-2.622513	-0.295364
O	3.803962	-0.420377	0.655073
O	3.144556	-0.812513	-1.668003
H	3.191481	0.342278	0.848889
H	2.579756	0.001533	-1.671779
S	1.158540	1.806420	-0.020431
O	1.706770	1.394334	-1.290405
O	2.005523	1.440730	1.114023
O	-0.217522	1.430085	0.223331
O	1.093586	3.382038	-0.050505
H	-1.595467	1.026376	-0.490238
H	1.922189	3.738652	-0.395515
C	-2.958284	-0.147162	0.106523
O	-2.506934	0.713492	-0.747905

O	-2.404492	-0.587800	1.082065
H	-0.768937	-0.468182	1.737877
C	-4.399015	-0.581208	-0.248496
F	-5.222391	0.452065	-0.101515
F	-4.800089	-1.556915	0.544141
F	-4.465795	-0.995967	-1.505530
N	0.184080	-0.577425	2.133072
H	0.594400	0.347743	2.279964
H	0.789030	-1.047723	1.421319
H	0.157561	-1.111986	2.995462

$(SA)_2 \cdot (NH_3)_2 \cdot (TFA)_1$

Atoms	X	Y	Z
S	-3.062686	-0.257713	-0.057659
O	-2.722635	0.724475	-1.100399
O	-4.372116	-0.786390	-0.127382
O	-2.963332	0.519645	1.313787
O	-1.984671	-1.269521	0.006462
H	-2.173353	1.099036	1.289379
H	-1.025398	-1.289630	-1.391746
S	1.960501	-1.749144	0.020145
O	1.138165	-0.547287	-0.039244
O	1.735105	-2.622987	-1.107656
O	1.880056	-2.375682	1.328039
O	3.466883	-1.295468	-0.168352
H	0.487290	-1.664319	2.068690
H	3.761888	-0.819147	0.617373
C	0.082190	1.787949	0.008219
O	-0.477646	1.641127	1.074514
O	-0.429738	1.655907	-1.164750
H	-1.423198	1.317091	-1.112311
C	1.546552	2.278489	-0.018202
F	1.534840	3.612131	0.003733
F	2.192031	1.889656	-1.102363
F	2.205039	1.858235	1.051962
N	-0.356294	-1.231943	-2.197433
H	0.022613	-0.283232	-2.193016
H	-0.823278	-1.435919	-3.074786
H	0.433009	-1.885016	-1.997343
N	-0.361800	-1.072611	2.211995
H	-0.079710	-0.091194	2.140709
H	-0.821524	-1.256007	3.097776
H	-1.016930	-1.239453	1.413323

$(SA)_2 \cdot (NH_3)_3 \cdot (TFA)_1$

Atoms	X	Y	Z
S	-3.045278	-0.997341	-0.154993
O	-2.034547	-1.984163	0.253015
O	-2.567035	-0.307982	-1.369035
O	-3.050323	0.117248	0.965518
O	-4.378965	-1.478519	-0.222962
H	-2.118097	0.440952	1.111384
H	0.007042	-0.700850	2.270989
S	0.156836	1.736951	0.343041
O	-0.628792	2.910046	0.017504
O	1.379163	2.274744	1.124827
O	0.655015	1.022906	-0.822083
O	-0.564787	0.827875	1.248469
H	0.183669	-0.486307	-1.353649
H	-3.712672	2.325584	-0.349416
C	2.474022	-0.831863	0.580272
O	1.914166	-1.938100	0.404262
O	2.398184	-0.092295	1.564336
H	1.968554	1.499205	1.341208
C	3.384356	-0.377353	-0.591884
F	3.622174	0.921985	-0.571090
F	2.835990	-0.683376	-1.775765
F	4.554891	-1.014574	-0.525774
N	-0.038563	-1.724363	2.189571
H	-0.919206	-1.952575	1.700147
H	0.025359	-2.173483	3.095823
H	0.782308	-1.979796	1.559289
N	0.028399	-1.499722	-1.571592
H	-0.754620	-1.820539	-0.972043
H	0.890508	-1.989771	-1.315612
H	-0.215784	-1.614672	-2.549160
N	-2.987545	2.275042	-1.060855
H	-2.856151	1.244251	-1.308870
H	-2.073325	2.619080	-0.654229
H	-3.252941	2.823361	-1.871983

Table S2. Atoms in molecules (AIM) topological parameters for the stable clusters obtained at the M06-2X/6-311++G(3df,3pd) level.

Clusters	Bonds	r (Å)	ρ (a.u.)	$\nabla^2\rho$(a.u.)
$(SA)_1\cdot(NH_3)_1\cdot(TFA)_1$	C=O···H-N	1.729	0.0416	0.1114
	S=O···H-N	1.534	0.0728	0.0943
	S=O···H-O	1.501	0.0738	0.1012
$(SA)_1\cdot(NH_3)_2\cdot(TFA)_1$	C=O···H-N	1.634	0.0584	0.0939
	S=O···H-N	1.754	0.0405	0.1171
	S=O···H-N	2.227	0.0152	0.0585
	C=O···H-N	1.543	0.0693	0.0994
	S=O···H-N	1.695	0.0476	0.1128
$(SA)_1\cdot(NH_3)_1\cdot(TFA)_2$	S=O···H-O	1.581	0.0584	0.1091
	S=O···H-O	1.557	0.0638	0.1077
	C=O···H-N	2.174	0.0163	0.0787
	S=O···H-N	1.634	0.0553	0.1045
	C=O···H-N	1.818	0.0326	0.1139
$(SA)_2\cdot(NH_3)_1\cdot(TFA)_1$	S=O···H-O	1.603	0.0528	0.1235
	S=O···H-O	1.687	0.0433	0.1193
	S=O···H-O	1.638	0.0515	0.1129
	S=O···H-N	2.132	0.0180	0.0714
	S=O···H-N	1.664	0.0474	0.1198

	C=O···H-N	1.766	0.0372	0.1116
$(SA)_1 \cdot (NH_3)_2 \cdot (TFA)_2$	S=O···H-N	1.679	0.0494	0.1131
	C=O···H-N	1.758	0.0403	0.1176
	C=O···H-N	2.208	0.0154	0.0662
	C=O···H-O	1.727	0.0385	0.1301
	S=O···H-O	1.480	0.0799	0.0909
	S=O···H-N	1.631	0.0531	0.1135
	C=O···H-N	1.586	0.0644	0.0924
$(SA)_2 \cdot (NH_3)_2 \cdot (TFA)_1$	C=O···H-N	2.073	0.0177	0.0747
	C=O···H-O	1.793	0.0349	0.1142
	S=O···H-O	1.428	0.0907	0.0812
	S=O···H-N	1.730	0.0436	0.1117
	S=O···H-N	1.708	0.0448	0.1107
	S=O···H-N	1.741	0.0423	0.1136
	S=O···H-N	1.696	0.0468	0.1069
$(SA)_1 \cdot (NH_3)_3 \cdot (TFA)_2$	C=O···H-N	1.587	0.0647	0.0912
	C=O···H-N	1.598	0.0597	0.1019
	S=O...H-N	1.772	0.0389	0.1089
	S=O...H-N	1.614	0.0595	0.1092
	C=O···H-N	1.945	0.0249	0.0988

	C=O···H-N	1.504	0.0760	0.0995
	C=O···H-N	1.668	0.0537	0.0967
	S=O···H-N	1.754	0.0380	0.1149
$(SA)_2 \cdot (NH_3)_3 \cdot (TFA)_1$	S=O···H-N	1.619	0.0570	0.1053
	S=O···H-N	1.580	0.0644	0.0995
	S=O···H-O	1.607	0.0559	0.1139
	S=O···H-N	1.668	0.0484	0.1149
	C=O···H-O	1.664	0.0485	0.1169
	S=O···H-N	1.926	0.0257	0.1066
	S=O···H-N	1.779	0.0383	0.1114
	S=O···H-N	1.827	0.0321	0.1143
	C=O···H-N	2.002	0.0235	0.0958
	C=O···H-N	1.618	0.0610	0.0933
$(TFA)_1 \cdot (NH_3)_1$	C=O···H-N	2.501	0.0105	0.0377
	H-N···H-O	1.646	0.0632	0.0591
$(TFA)_2 \cdot (NH_3)_1$	H-N···H-O	1.483	0.0937	0.0086
	C=O···H-N	1.984	0.0213	0.0863
	C=O···H-O	1.687	0.0406	0.1331
$(TFA)_2 \cdot (NH_3)_2$	C=O···H-N	1.567	0.0689	0.0869
	C=O···H-N	1.608	0.0584	0.1028

	C=O···H-N	1.608	0.0584	0.1028
	C=O···H-N	1.567	0.0689	0.0869
$(TFA)_3 \cdot (NH_3)_1$	C=O···H-O	1.515	0.0712	0.1045
	C=O···H-O	1.514	0.0715	0.1037
	C=O···H-N	1.734	0.0405	0.1123
	C=O···H-N	1.739	0.0399	0.1129
$(TFA)_3 \cdot (NH_3)_2$	C=O···H-O	1.400	0.0997	0.0544
	C=O···H-N	1.843	0.0304	0.1089
	C=O···H-N	1.679	0.0488	0.1115
	C=O···H-N	1.572	0.0650	0.1024
	C=O···H-N	1.577	0.0672	0.0862
	C=O···H-N	1.920	0.0267	0.1035
$(TFA)_3 \cdot (NH_3)_3$	C=O···H-N	1.684	0.0516	0.0935
	C=O···H-N	1.896	0.0285	0.1099
	C=O···H-N	1.893	0.0284	0.1108
	C=O···H-N	1.629	0.0572	0.1028
	C=O···H-N	1.685	0.0515	0.0938
	C=O···H-N	1.818	0.0330	0.1116

Table S3. Proton-transfer parameter (ρ_{PT}, Å) and the total number of proton transfers (n) for $(SA)_x\cdot(NH_3)_y\cdot(TFA)_z$ ($0 \le y \le x+z \le 3$, $z = 1, 2, 3$). r_{OH} and $r_{H\cdots N}$ are the bond distances between the O and H atoms and that between the H and N atoms, respectively.

Clusters	r_{OH} (Å)	$r_{N\ldots H}$ (Å)	ρ_{PT} (Å)	Proton donor	n
$(SA)_1\cdot(NH_3)_1\cdot(TFA)_1$	1.534	1.080	0.512	SA	1
$(SA)_1\cdot(NH_3)_2\cdot(TFA)_1$	1.695	1.047	0.706	SA	2
	1.634	1.062	0.629	TFA	
$(SA)_1\cdot(NH_3)_1\cdot(TFA)_2$	1.634	1.056	0.636	SA	1
$(SA)_2\cdot(NH_3)_1\cdot(TFA)_1$	2.132	1.023	1.167	SA	1
$(SA)_1\cdot(NH_3)_2\cdot(TFA)_2$	1.679	1.050	0.687	SA	2
	1.586	1.069	0.574	TFA	
$(SA)_2\cdot(NH_3)_2\cdot(TFA)_1$	1.696	1.049	0.705	SA	2
	1.730	1.045	0.743	SA	
$(SA)_1\cdot(NH_3)_3\cdot(TFA)_2$	1.772	1.039	0.791	SA	3
	1.587	1.072	0.572	TFA	
	1.668	1.056	0.669	TFA	
$(SA)_2\cdot(NH_3)_3\cdot(TFA)_1$	1.668	1.048	0.678	SA	3
	1.580	1.068	0.570	SA	
	1.618	1.066	0.609	TFA	
$(TFA)_1\cdot(NH_3)_1$	1.020	1.646	-0.569	TFA	0
$(TFA)_2\cdot(NH_3)_1$	1.074	1.483	-0.352	TFA	0
$(TFA)_2\cdot(NH_3)_2$	1.567	1.075	0.549	TFA	2
	1.567	1.075	0.549	TFA	
$(TFA)_3\cdot(NH_3)_1$	1.734	1.041	0.750	TFA	1
$(TFA)_3\cdot(NH_3)_2$	1.577	1.074	0.560	TFA	2
	1.679	1.049	0.687	TFA	
$(TFA)_3\cdot(NH_3)_3$	1.672	1.058	0.671	TFA	3
	1.684	1.058	0.683	TFA	
	1.893	1.033	0.917	TFA	

Table S4. Gibbs free formation energies (ΔG, kcal mol^{-1}) of the studied clusters at different temperatures at the RI-CC2/aug-cc-pV(T + d)Z//M06-2X/6-311++G(3df,3pd) level of theory.

Clusters	ΔG (kcal mol^{-1})		
	240 K	230 K	220 K
$(TFA)_2$	-7.27	-7.64	-8.02
$(TFA)_3$	-6.71	-7.43	-8.18
$(SA)_1 \cdot (TFA)_1$	-9.24	-9.58	-9.94
$(SA)_1 \cdot (TFA)_2$	-16.58	-17.35	-18.13
$(SA)_2 \cdot (TFA)_1$	-17.86	-18.65	-19.45
$(SA)_2$	-10.39	-10.73	-11.07
$(SA)_3$	-18.41	-19.18	-19.96
$(SA)_2 \cdot (NH_3)_1$	-27.22	-28.00	-28.77
$(SA)_2 \cdot (NH_3)_2$	-39.03	-40.15	-41.27
$(SA)_3 \cdot (NH_3)_1$	-39.87	-41.04	-42.21
$(SA)_3 \cdot (NH_3)_2$	-57.10	-58.63	-60.17
$(SA)_3 \cdot (NH_3)_3$	-72.56	-74.48	-76.40
$(SA)_1 \cdot (NH_3)_1$	-9.12	-9.42	-9.73
$(SA)_1 \cdot (NH_3)_1 \cdot (TFA)_1$	-19.27	-20.00	-20.74
$(SA)_1 \cdot (NH_3)_2 \cdot (TFA)_1$	-29.72	-30.79	-31.86
$(SA)_1 \cdot (NH_3)_1 \cdot (TFA)_2$	-28.76	-29.95	-31.15
$(SA)_1 \cdot (NH_3)_2 \cdot (TFA)_2$	-39.23	-40.84	-42.47
$(SA)_1 \cdot (NH_3)_3 \cdot (TFA)_2$	-46.73	-48.67	-50.63
$(NH_3)_1 \cdot (TFA)_1$	-6.26	-6.56	-6.88
$(SA)_2 \cdot (NH_3)_1 \cdot (TFA)_1$	-36.44	-37.56	-38.69
$(SA)_2 \cdot (NH_3)_2 \cdot (TFA)_1$	-47.97	-49.57	-51.18
$(SA)_2 \cdot (NH_3)_3 \cdot (TFA)_1$	-63.14	-65.12	-67.11
$(NH_3)_1 \cdot (TFA)_2$	-12.76	-13.40	-14.05
$(NH_3)_2 \cdot (TFA)_2$	-18.32	-19.42	-20.53
$(NH_3)_1 \cdot (TFA)_3$	-19.77	-20.90	-22.05
$(NH_3)_2 \cdot (TFA)_3$	-33.47	-34.96	-36.47
$(NH_3)_3 \cdot (TFA)_3$	-40.74	-42.80	-44.88

Table S5. Gibbs free formation energies (ΔG, kcal mol^{-1}) with a scaling factor of 0.97 for Zero-Point Energies of the studied clusters at different temperatures at the RI-CC2/aug-cc-pV(T + d)Z//M06-2X/6-311++G(3df,3pd) level of theory. p = 1 atm.

Clusters	ΔG (kcal mol^{-1})		
	240 K	230 K	220 K
$(TFA)_2$	-6.16	-6.62	-7.08
$(TFA)_3$	-4.50	-5.41	-6.31
$(SA)_1 \cdot (TFA)_1$	-8.54	-8.96	-9.37
$(SA)_1 \cdot (TFA)_2$	-15.13	-16.04	-16.94
$(SA)_2 \cdot (TFA)_1$	-17.05	-17.95	-18.84
$(SA)_2$	-9.90	-10.29	-10.68
$(SA)_3$	-17.72	-18.58	-19.45
$(SA)_2 \cdot (NH_3)_1$	-27.94	-28.72	-29.50
$(SA)_2 \cdot (NH_3)_2$	-39.93	-41.07	-42.21
$(SA)_3 \cdot (NH_3)_1$	-40.14	-41.36	-42.59
$(SA)_3 \cdot (NH_3)_2$	-57.80	-59.39	-60.98
$(SA)_3 \cdot (NH_3)_3$	-74.09	-76.03	-77.98
$(SA)_1 \cdot (NH_3)_1$	-9.42	-9.73	-10.04
$(SA)_1 \cdot (NH_3)_1 \cdot (TFA)_1$	-19.24	-20.03	-20.81
$(SA)_1 \cdot (NH_3)_2 \cdot (TFA)_1$	-29.73	-30.86	-31.99
$(SA)_1 \cdot (NH_3)_1 \cdot (TFA)_2$	-28.58	-29.85	-31.13
$(SA)_1 \cdot (NH_3)_2 \cdot (TFA)_2$	-39.91	-41.57	-43.24
$(SA)_1 \cdot (NH_3)_3 \cdot (TFA)_2$	-47.12	-49.15	-51.18
$(NH_3)_1 \cdot (TFA)_1$	-6.45	-6.78	-7.10
$(SA)_2 \cdot (NH_3)_1 \cdot (TFA)_1$	-35.86	-37.09	-38.32
$(SA)_2 \cdot (NH_3)_2 \cdot (TFA)_1$	-48.82	-50.46	-52.10
$(SA)_2 \cdot (NH_3)_3 \cdot (TFA)_1$	-64.47	-66.49	-68.50
$(NH_3)_1 \cdot (TFA)_2$	-11.35	-12.11	-12.87
$(NH_3)_2 \cdot (TFA)_2$	-18.08	-19.25	-20.42
$(NH_3)_1 \cdot (TFA)_3$	-18.26	-19.54	-20.82
$(NH_3)_2 \cdot (TFA)_3$	-32.14	-33.78	-35.42
$(NH_3)_3 \cdot (TFA)_3$	-42.04	-44.13	-46.21

Table S6. Collision coefficients (β, $cm^3\ s^{-1}$) for each cluster in the present study.

Collisions	β ($cm^3\ s^{-1}$)		
	240 K	230 K	220 K
SA+SA	1.57×10^{-10}	1.54×10^{-10}	1.51×10^{-10}
$(SA)_2$+SA	2.36×10^{-10}	2.31×10^{-10}	2.26×10^{-10}
SA+TFA	1.83×10^{-10}	1.79×10^{-10}	1.75×10^{-10}
$(SA)_2$+TFA	2.59×10^{-10}	2.53×10^{-10}	2.48×10^{-10}
TFA+TFA	2.08×10^{-10}	2.04×10^{-10}	1.99×10^{-10}
$(TFA)_2$+SA	2.87×10^{-10}	2.81×10^{-10}	2.75×10^{-10}
$(TFA)_2$+TFA	3.10×10^{-10}	3.04×10^{-10}	2.97×10^{-10}
$(TFA)_3$+SA	3.13×10^{-10}	3.06×10^{-10}	2.99×10^{-10}
$(SA)_1\cdot(TFA)_1$+SA	2.58×10^{-10}	2.53×10^{-10}	2.47×10^{-10}
$(SA)_1\cdot(TFA)_1$+TFA	2.81×10^{-10}	2.75×10^{-10}	2.69×10^{-10}
$(SA)_1\cdot(NH_3)_1\cdot(TFA)_1$+SA	2.73×10^{-10}	2.67×10^{-10}	2.61×10^{-10}
TFA+$(SA)_1\cdot(NH_3)_1\cdot(TFA)_1$	2.95×10^{-10}	2.89×10^{-10}	2.83×10^{-10}
$(SA)_1\cdot(NH_3)_2\cdot(TFA)_1$+SA	2.91×10^{-10}	2.84×10^{-10}	2.78×10^{-10}
TFA+$(SA)_1\cdot(NH_3)_2\cdot(TFA)_1$	3.13×10^{-10}	3.06×10^{-10}	2.99×10^{-10}
$(SA)_2\cdot(TFA)_1$+SA	3.57×10^{-10}	3.50×10^{-10}	3.42×10^{-10}
$(SA)_2\cdot(NH_3)_1\cdot(TFA)_1$+SA	3.29×10^{-10}	3.22×10^{-10}	3.15×10^{-10}
$(SA)_2\cdot(NH_3)_2\cdot(TFA)_1$+SA	2.67×10^{-10}	2.62×10^{-10}	2.56×10^{-10}
$(SA)_1\cdot(TFA)_2$+SA	4.20×10^{-10}	4.11×10^{-10}	4.02×10^{-10}
$(SA)_1\cdot(NH_3)_1\cdot(TFA)_2$+SA	2.61×10^{-10}	2.55×10^{-10}	2.50×10^{-10}
$(SA)_1\cdot(NH_3)_2\cdot(TFA)_2$+SA	2.67×10^{-10}	2.62×10^{-10}	2.56×10^{-10}
NH_3+SA	2.04×10^{-10}	2.00×10^{-10}	1.96×10^{-10}
NH_3+$(SA)_2$	3.72×10^{-10}	3.64×10^{-10}	3.56×10^{-10}
NH_3+$(SA)_3$	5.31×10^{-10}	5.20×10^{-10}	5.09×10^{-10}
NH_3+TFA	2.52×10^{-10}	2.46×10^{-10}	2.41×10^{-10}
$(TFA)_2$+NH_3	4.75×10^{-10}	4.65×10^{-10}	4.55×10^{-10}
$(TFA)_3$+NH_3	5.47×10^{-10}	5.36×10^{-10}	5.24×10^{-10}
$(SA)_1\cdot(TFA)_1$+NH_3	4.17×10^{-10}	4.08×10^{-10}	3.99×10^{-10}
NH_3+$(SA)_1\cdot(NH_3)_1\cdot(TFA)_1$	4.48×10^{-10}	4.39×10^{-10}	4.29×10^{-10}
$(SA)_2\cdot(TFA)_1$+NH_3	6.28×10^{-10}	6.15×10^{-10}	6.01×10^{-10}
$(SA)_2\cdot(NH_3)_1\cdot(TFA)_1$+$NH_3$	5.76×10^{-10}	5.64×10^{-10}	5.51×10^{-10}
$(SA)_2\cdot(NH_3)_2\cdot(TFA)_1$+$NH_3$	4.59×10^{-10}	4.50×10^{-10}	4.40×10^{-10}
$(SA)_1\cdot(TFA)_2$+NH_3	7.55×10^{-10}	7.39×10^{-10}	7.23×10^{-10}
$(SA)_1\cdot(NH_3)_1\cdot(TFA)_2$+$NH_3$	4.47×10^{-10}	4.37×10^{-10}	4.28×10^{-10}
$(SA)_1\cdot(NH_3)_2\cdot(TFA)_2$+$NH_3$	4.62×10^{-10}	4.52×10^{-10}	4.42×10^{-10}
$(SA)_1\cdot(NH_3)_1$+SA	2.18×10^{-10}	2.13×10^{-10}	2.09×10^{-10}
$(SA)_1\cdot(NH_3)_1$+TFA	2.45×10^{-10}	2.39×10^{-10}	2.34×10^{-10}
$(SA)_2\cdot(NH_3)_1$+SA	2.55×10^{-10}	2.50×10^{-10}	2.45×10^{-10}
$(SA)_2\cdot(NH_3)_1$+TFA	2.78×10^{-10}	2.72×10^{-10}	2.66×10^{-10}
$(SA)_2\cdot(NH_3)_1$+NH_3	4.12×10^{-10}	4.04×10^{-10}	3.95×10^{-10}
$(SA)_3\cdot(NH_3)_1$+NH_3	4.20×10^{-10}	4.11×10^{-10}	4.02×10^{-10}
$(NH_3)_1\cdot(TFA)_1$+SA	2.38×10^{-10}	2.33×10^{-10}	2.28×10^{-10}
$(NH_3)_1\cdot(TFA)_1$+TFA	2.64×10^{-10}	2.58×10^{-10}	2.53×10^{-10}

$(NH_3)_1 \cdot (TFA)_2$+SA	3.12×10^{-10}	3.06×10^{-10}	2.99×10^{-10}
$(NH_3)_1 \cdot (TFA)_2$+TFA	3.35×10^{-10}	3.28×10^{-10}	3.20×10^{-10}
$(NH_3)_1 \cdot (TFA)_2$+NH_3	5.26×10^{-10}	5.15×10^{-10}	5.04×10^{-10}
$(NH_3)_1 \cdot (TFA)_3$+SA	3.79×10^{-10}	3.71×10^{-10}	3.63×10^{-10}
$(NH_3)_1 \cdot (TFA)_3$+NH_3	6.80×10^{-10}	6.66×10^{-10}	6.51×10^{-10}
$(SA)_2 \cdot (NH_3)_2$+SA	2.59×10^{-10}	2.54×10^{-10}	2.48×10^{-10}
$(SA)_2 \cdot (NH_3)_2$+TFA	2.81×10^{-10}	2.75×10^{-10}	2.69×10^{-10}
$(SA)_3 \cdot (NH_3)_2$+NH_3	5.63×10^{-10}	5.51×10^{-10}	5.39×10^{-10}
$(NH_3)_2 \cdot (TFA)_2$+SA	3.04×10^{-10}	2.98×10^{-10}	2.91×10^{-10}
$(NH_3)_2 \cdot (TFA)_2$+TFA	3.26×10^{-10}	3.19×10^{-10}	3.12×10^{-10}
$(SA)_3 \cdot (NH_3)_3$+SA	2.99×10^{-10}	2.93×10^{-10}	2.86×10^{-10}
$(SA)_2 \cdot (NH_3)_3 \cdot (TFA)_1$+SA	3.01×10^{-10}	2.95×10^{-10}	2.88×10^{-10}
$(NH_3)_3 \cdot (TFA)_3$+SA	2.71×10^{-10}	2.65×10^{-10}	2.59×10^{-10}
$(NH_3)_2 \cdot (TFA)_3$+SA	2.87×10^{-10}	2.81×10^{-10}	2.75×10^{-10}
$(NH_3)_2 \cdot (TFA)_3$+NH_3	5.03×10^{-10}	4.92×10^{-10}	3.31×10^{-10}
$(SA)_1 \cdot (NH_3)_3 \cdot (TFA)_2$+SA	2.99×10^{-10}	2.93×10^{-10}	2.86×10^{-10}

Table S7. Total evaporation coefficients ($\Sigma\gamma$, s^{-1}) of each cluster in the present study.

Clusters	$\Sigma\gamma$ (s^{-1})		
	240 K	230 K	220 K
$(SA)_2$	8.32×10^{-1}	1.57×10^{-1}	2.53×10^{-2}
$(SA)_3$	3.59×10^{2}	6.89×10^{1}	1.11×10^{1}
$(TFA)_2$	7.63×10^{2}	1.79×10^{2}	3.58×10^{1}
$(TFA)_3$	3.07×10^{10}	1.53×10^{10}	6.87×10^{9}
$(SA)_1\cdot(TFA)_1$	2.15×10^{1}	4.5	7.79×10^{-1}
$(SA)_1\cdot(NH_3)_1\cdot(TFA)_1$	9.39	1.64	2.49×10^{-1}
$(SA)_1\cdot(NH_3)_2\cdot(TFA)_1$	4.18	7.83×10^{-1}	1.29×10^{-1}
$(SA)_2\cdot(TFA)_1$	1.25×10^{3}	2.41×10^{2}	3.92×10^{1}
$(SA)_2\cdot(NH_3)_1\cdot(TFA)_1$	3.42×10^{1}	7.17	1.24
$(SA)_2\cdot(NH_3)_2\cdot(TFA)_1$	6.22×10^{1}	9.84	1.29
$(SA)_1\cdot(TFA)_2$	1.78×10^{3}	3.64×10^{2}	6.57×10^{1}
$(SA)_1\cdot(NH_3)_1\cdot(TFA)_2$	2.06×10^{1}	3.24	4.30×10^{-1}
$(SA)_1\cdot(NH_3)_2\cdot(TFA)_2$	2.09×10^{1}	2.76	2.88×10^{-1}
$(SA)_1\cdot(NH_3)_1$	3.10×10^{1}	7.15	1.41
$(SA)_2\cdot(NH_3)_1$	5.38×10^{-6}	4.52×10^{-7}	3.11×10^{-8}
$(SA)_3\cdot(NH_3)_1$	2.36×10^{-2}	3.25×10^{-3}	3.64×10^{-4}
$(NH_3)_1\cdot(TFA)_1$	1.53×10^{4}	4.59×10^{3}	1.18×10^{3}
$(NH_3)_1\cdot(TFA)_2$	1.46×10^{5}	4.99×10^{4}	1.55×10^{4}
$(NH_3)_1\cdot(TFA)_3$	4.23×10^{3}	7.81×10^{2}	1.21×10^{2}
$(SA)_2\cdot(NH_3)_2$	2.22×10^{-1}	3.67×10^{-2}	5.04×10^{-3}
$(SA)_3\cdot(NH_3)_2$	2.62×10^{-6}	2.53×10^{-7}	1.93×10^{-8}
$(NH_3)_2\cdot(TFA)_2$	1.39×10^{5}	3.13×10^{4}	6.14×10^{3}
$(SA)_3\cdot(NH_3)_3$	1.44×10^{-4}	1.53×10^{-5}	1.36×10^{-6}
$(SA)_2\cdot(NH_3)_3\cdot(TFA)_1$	2.16×10^{-4}	2.41×10^{-5}	2.20×10^{-6}
$(SA)_1\cdot(NH_3)_3\cdot(TFA)_2$	2.09×10^{3}	5.23×10^{2}	1.15×10^{2}
$(NH_3)_3\cdot(TFA)_3$	3.69×10^{3}	5.58×10^{2}	7.10×10^{1}
$(NH_3)_2\cdot(TFA)_3$	6.96×10^{-3}	9.28×10^{-4}	1.03×10^{-4}

Table S8. Ratios ($\beta C/\Sigma\gamma$) between monomer molecule collisions and evaporation coefficients of each cluster involving TFA in the present study. [SA] = 7.0×10^{5} molecules cm^{-3}, [NH_3] = 1.0×10^{10} molecules cm^{-3}, [TFA] = 1.0×10^{6} molecules cm^{-3}.

Clusters	$\beta C/\Sigma\gamma$		
	240 K	230 K	220 K
Collision with SA monomer: C = [SA]			
$(SA)_2$	1.98×10^{-4}	1.03×10^{-3}	6.24×10^{-3}
$(TFA)_2$	2.64×10^{-7}	1.10×10^{-6}	5.38×10^{-6}
$(TFA)_3$	7.13×10^{-15}	1.40×10^{-14}	3.05×10^{-14}
$(SA)_1\cdot(TFA)_1$	8.40×10^{-6}	3.93×10^{-5}	2.22×10^{-4}
$(SA)_1\cdot(NH_3)_1\cdot(TFA)_1$	2.03×10^{-5}	1.14×10^{-4}	7.34×10^{-4}
$(SA)_1\cdot(NH_3)_2\cdot(TFA)_1$	4.87×10^{-5}	2.54×10^{-4}	1.51×10^{-3}
$(SA)_2\cdot(TFA)_1$	2.00×10^{-7}	1.01×10^{-6}	6.11×10^{-6}
$(SA)_2\cdot(NH_3)_1\cdot(TFA)_1$	6.73×10^{-6}	3.14×10^{-5}	1.77×10^{-4}
$(SA)_2\cdot(NH_3)_2\cdot(TFA)_1$	3.01×10^{-6}	1.86×10^{-5}	1.39×10^{-4}
$(SA)_1\cdot(TFA)_2$	1.65×10^{-7}	7.92×10^{-6}	4.29×10^{-6}
$(SA)_1\cdot(NH_3)_1\cdot(TFA)_2$	8.86×10^{-6}	5.52×10^{-5}	4.07×10^{-4}
$(SA)_1\cdot(NH_3)_2\cdot(TFA)_2$	8.94×10^{-6}	6.64×10^{-5}	6.21×10^{-4}
$(SA)_1\cdot(NH_3)_1$	4.92×10^{-6}	2.09×10^{-5}	1.03×10^{-4}
$(SA)_2\cdot(NH_3)_1$	3.33×10^{1}	3.87×10^{2}	5.51×10^{3}
$(NH_3)_1\cdot(TFA)_1$	1.08×10^{-8}	3.55×10^{-8}	1.35×10^{-7}
$(NH_3)_1\cdot(TFA)_2$	1.50×10^{-9}	4.28×10^{-9}	1.35×10^{-8}
$(NH_3)_1\cdot(TFA)_3$	6.26×10^{-8}	3.32×10^{-7}	2.21×10^{-6}
$(SA)_2\cdot(NH_3)_2$	8.17×10^{-4}	4.83×10^{-3}	3.45×10^{-2}
$(NH_3)_2\cdot(TFA)_2$	1.53×10^{-9}	6.66×10^{-9}	3.32×10^{-8}
$(SA)_3\cdot(NH_3)_3$	1.45	1.34×10^{1}	1.48×10^{2}
$(SA)_2\cdot(NH_3)_3\cdot(TFA)_1$	9.77×10^{-1}	8.57	9.18×10^{1}
$(SA)_1\cdot(NH_3)_3\cdot(TFA)_2$	1.00×10^{-7}	3.91×10^{-7}	1.73×10^{-6}
$(NH_3)_3(TFA)_3$	5.14×10^{-8}	3.33×10^{-7}	2.56×10^{-6}
$(NH_3)_2(TFA)_3$	2.89×10^{-2}	2.12×10^{-1}	1.87
Collision with NH_3 monomer: C = [NH_3]			
$(SA)_2$	4.47	2.32×10^{1}	1.41×10^{2}
$(SA)_3$	1.48×10^{-2}	7.55×10^{-2}	4.58×10^{-1}
$(TFA)_2$	6.23×10^{-3}	2.60×10^{-2}	1.27×10^{-1}
$(TFA)_3$	1.78×10^{-10}	3.49×10^{-10}	7.63×10^{-10}
$(SA)_1\cdot(TFA)_1$	1.94×10^{-1}	9.07×10^{-1}	5.13
$(SA)_1\cdot(NH_3)_1\cdot(TFA)_1$	4.78×10^{-1}	2.68	1.72×10^{1}
$(SA)_2\cdot(TFA)_1$	5.03×10^{-3}	2.55×10^{-2}	1.53×10^{-1}
$(SA)_2\cdot(NH_3)_1\cdot(TFA)_1$	1.68×10^{-1}	7.87×10^{-1}	4.44
$(SA)_2\cdot(NH_3)_2\cdot(TFA)_1$	7.39×10^{-2}	4.57×10^{-1}	3.42
$(SA)_1\cdot(TFA)_2$	4.24×10^{-3}	2.03×10^{-2}	1.10×10^{-1}
$(SA)_1\cdot(NH_3)_1\cdot(TFA)_2$	2.17×10^{-1}	1.35	9.95
$(SA)_1\cdot(NH_3)_2\cdot(TFA)_2$	2.21×10^{-1}	1.64	1.53×10^{1}
$(SA)_2\cdot(NH_3)_1$	7.67×10^{5}	8.92×10^{6}	1.27×10^{8}

$(SA)_3 \cdot (NH_3)_1$	1.77×10^{2}	1.26×10^{3}	1.10×10^{4}
$(NH_3)_1 \cdot (TFA)_2$	3.61×10^{-5}	1.03×10^{-4}	3.24×10^{-4}
$(NH_3)_1 \cdot (TFA)_3$	1.61×10^{-3}	8.52×10^{-3}	5.39×10^{-2}
$(SA)_3 \cdot (NH_3)_2$	2.15×10^{6}	2.18×10^{7}	2.79×10^{8}
$(NH_3)_2 \cdot (TFA)_3$	7.22×10^{2}	5.3×10^{3}	3.22×10^{4}
Collision with TFA monomer: C = [TFA]			
$(SA)_2$	3.11×10^{-4}	1.62×10^{-3}	9.79×10^{-3}
$(TFA)_2$	4.07×10^{-7}	1.70×10^{-6}	8.29×10^{-6}
$(SA)_1 \cdot (TFA)_1$	1.31×10^{-5}	6.12×10^{-5}	3.46×10^{-4}
$(SA)_1 \cdot (NH_3)_1 \cdot (TFA)_1$	3.15×10^{-5}	1.77×10^{-4}	1.14×10^{-3}
$(SA)_1 \cdot (NH_3)_2 \cdot (TFA)_1$	7.48×10^{-5}	3.91×10^{-4}	2.33×10^{-3}
$(SA)_1 \cdot (NH_3)_1$	7.89×10^{-6}	3.35×10^{-5}	1.66×10^{-4}
$(SA)_2 \cdot (NH_3)_1$	5.17×10^{1}	6.02×10^{2}	8.58×10^{3}
$(NH_3)_1 \cdot (TFA)_1$	1.72×10^{-8}	5.63×10^{-8}	2.15×10^{-7}
$(NH_3)_1 \cdot (TFA)_2$	2.30×10^{-9}	6.56×10^{-9}	2.06×10^{-8}
$(SA)_2 \cdot (NH_3)_2$	1.27×10^{-3}	7.50×10^{-3}	5.35×10^{-2}
$(NH_3)_2 \cdot (TFA)_2$	2.34×10^{-9}	1.02×10^{-8}	5.08×10^{-8}

Table S9. Contributions of different formation pathways of $(SA)_3 \cdot (NH_3)_3$ and $(SA)_2 \cdot (NH_3)_3 \cdot (TFA)_1$ clusters to the main cluster formation pathway and the thermodynamic barriers (kcal mol^{-1}) of main pathway involving TFA [from $(SA)_1 \cdot (NH_3)_1$ cluster to $(SA)_1 \cdot (NH_3)_1 \cdot (TFA)_1$ cluster] at different nucleation precursor concentrations and different temperatures (T, 240 K, 230 K, and 220 K). CS = 2.0×10^{-2} s^{-1}.

T	Concentrations (molecules cm^{-3})			$(SA)_3 \cdot (NH_3)_3$	$(SA)_2 \cdot (NH_3)_3 \cdot (TFA)_1$	Others
240 K	$[NH_3]= 1.0\times10^{10}$ $[TFA]= 1.0\times10^{7}$	[SA]	7.0×10^{5}	92%	6%	2%
			1.0×10^{6}	91%	6%	3%
			1.0×10^{7}	89%	3%	8%
	$[SA]= 7.0\times10^{5}$ $[TFA]= 1.0\times10^{7}$	$[NH_3]$	1.0×10^{8}	100%	0%	0%
			1.0×10^{9}	99%	0%	1%
			1.0×10^{10}	92%	6%	2%
			1.0×10^{11}	65%	32%	3%
	$[SA]= 7.0\times10^{5}$ $[NH_3]= 1.0\times10^{11}$	[TFA]	1.0×10^{6}	73%	20%	7%
			1.0×10^{7}	65%	32%	3%
			1.0×10^{8}	43%	54%	3%
230 K	$[NH_3]= 1.0\times10^{10}$ $[TFA]= 1.0\times10^{7}$	[SA]	7.0×10^{5}	68%	27%	5%
			1.0×10^{6}	70%	27%	3%
			1.0×10^{7}	75%	16%	9%
	$[SA]= 7.0\times10^{5}$ $[TFA]= 1.0\times10^{7}$	$[NH_3]$	1.0×10^{8}	99%	0%	1%
			1.0×10^{9}	95%	4%	1%
			1.0×10^{10}	68%	27%	5%
			1.0×10^{11}	24%	61%	15%
	$[SA]= 7.0\times10^{5}$ $[NH_3]= 1.0\times10^{11}$	[TFA]	1.0×10^{6}	39%	45%	16%
			1.0×10^{7}	24%	61%	15%
			1.0×10^{8}	5%	87%	8%
220 K	$[NH_3]= 1.0\times10^{10}$ $[TFA]= 1.0\times10^{7}$	[SA]	7.0×10^{5}	20%	63%	17%
			1.0×10^{6}	21%	63%	18%
			1.0×10^{7}	33%	50%	17%
	$[SA]= 7.0\times10^{5}$ $[TFA]= 1.0\times10^{7}$	$[NH_3]$	1.0×10^{8}	96%	3%	1%
			1.0×10^{9}	68%	24%	8%
			1.0×10^{10}	20%	63%	17%
			1.0×10^{11}	16%	68%	16%
	$[SA]= 7.0\times10^{5}$ $[NH_3]= 1.0\times10^{11}$	[TFA]	1.0×10^{6}	28%	53%	19%
			1.0×10^{7}	16%	68%	16%
			1.0×10^{8}	2%	93%	5%

Table S10. Relative hydrate distributions of the clusters at varying relative humidities (RHs) at different temperatures.

Clusters	Relative hydrate distributions				
	RH=20%	RH=40%	RH=60%	RH=80%	RH=100%
			240 K		
SA	0.65	0.43	0.29	0.20	0.15
$(SA)_1 \cdot (H_2O)_1$	0.25	0.33	0.34	0.32	0.29
$(SA)_1 \cdot (H_2O)_2$	0.09	0.24	0.36	0.45	0.52
$(SA)_1 \cdot (H_2O)_3$	0.00	0.01	0.01	0.02	0.03
TFA	0.90	0.81	0.73	0.66	0.60
$(TFA)_1 \cdot (H_2O)_1$	0.10	0.17	0.24	0.28	0.32
$(TFA)_1 \cdot (H_2O)_2$	0.00	0.02	0.04	0.06	0.08
$(SA)_1 \cdot (TFA)_1$	0.63	0.41	0.28	0.20	0.15
$(SA)_1 \cdot (TFA)_1 \cdot (H_2O)_1$	0.30	0.39	0.40	0.38	0.36
$(SA)_1 \cdot (TFA)_1 \cdot (H_2O)_2$	0.08	0.20	0.32	0.41	0.48
$(SA)_1 \cdot (TFA)_1 \cdot (H_2O)_3$	0.00	0.00	0.00	0.01	0.01
NH_3	1.00	1.00	1.00	1.00	1.00
$(NH_3)_1 \cdot (H_2O)_2$	0.00	0.00	0.00	0.00	0.00
$(NH_3)_1 \cdot (H_2O)_2$	0.00	0.00	0.00	0.00	0.00
$(NH_3)_1 \cdot (TFA)_1$	0.99	0.99	0.98	0.98	0.97
$(NH_3)_1 \cdot (TFA)_1 \cdot (H_2O)_1$	0.01	0.01	0.02	0.02	0.03
$(NH_3)_1 \cdot (TFA)_1 \cdot (H_2O)_2$	0.00	0.00	0.00	0.00	0.00
$(SA)_1 \cdot (NH_3)_1$	0.36	0.12	0.05	0.03	0.02
$(SA)_1 \cdot (NH_3)_1 \cdot (H_2O)_1$	0.00	0.00	0.00	0.00	0.00
$(SA)_1 \cdot (NH_3)_1 \cdot (H_2O)_2$	0.62	0.81	0.84	0.83	0.81
$(SA)_1 \cdot (NH_3)_1 \cdot (H_2O)_3$	0.03	0.07	0.11	0.14	0.17
$(SA)_1 \cdot (NH_3)_1 \cdot (TFA)_1$	0.07	0.03	0.02	0.02	0.01
$(SA)_1 \cdot (NH_3)_1 \cdot (TFA)_1 \cdot (H_2O)_1$	0.89	0.88	0.84	0.80	0.76
$(SA)_1 \cdot (NH_3)_1 \cdot (TFA)_1 \cdot (H_2O)_2$	0.04	0.08	0.11	0.14	0.17
$(SA)_1 \cdot (NH_3)_1 \cdot (TFA)_1 \cdot (H_2O)_3$	0.00	0.01	0.02	0.04	0.06
$(SA)_1 \cdot (NH_3)_2 \cdot (TFA)_1$	0.38	0.16	0.07	0.04	0.02
$(SA)_1 \cdot (NH_3)_2 \cdot (TFA)_1 \cdot (H_2O)_1$	0.40	0.33	0.24	0.17	0.13
$(SA)_1 \cdot (NH_3)_2 \cdot (TFA)_1 \cdot (H_2O)_2$	0.15	0.24	0.26	0.25	0.23
$(SA)_1 \cdot (NH_3)_2 \cdot (TFA)_1 \cdot (H_2O)_3$	0.08	0.27	0.43	0.54	0.62
			230 K		
SA	0.64	0.41	0.28	0.20	0.14
$(SA)_1 \cdot (H_2O)_1$	0.26	0.34	0.34	0.32	0.29
$(SA)_1 \cdot (H_2O)_2$	0.09	0.24	0.37	0.46	0.53
$(SA)_1 \cdot (H_2O)_3$	0.00	0.01	0.02	0.03	0.04
TFA	0.90	0.81	0.73	0.67	0.60
$(TFA)_1 \cdot (H_2O)_1$	0.09	0.17	0.23	0.28	0.32
$(TFA)_1 \cdot (H_2O)_2$	0.00	0.02	0.03	0.05	0.08
$(SA)_1 \cdot (TFA)_1$	0.60	0.38	0.26	0.18	0.14
$(SA)_1 \cdot (TFA)_1 \cdot (H_2O)_1$	0.31	0.39	0.40	0.38	0.35
$(SA)_1 \cdot (TFA)_1 \cdot (H_2O)_2$	0.09	0.22	0.34	0.43	0.50
$(SA)_1 \cdot (TFA)_1 \cdot (H_2O)_3$	0.00	0.00	0.00	0.01	0.01
NH_3	1.00	1.00	1.00	1.00	1.00
$(NH_3)_1 \cdot (H_2O)_2$	0.00	0.00	0.00	0.00	0.00
$(NH_3)_1 \cdot (H_2O)_2$	0.00	0.00	0.00	0.00	0.00
$(NH_3)_1 \cdot (TFA)_1$	1.00	0.99	0.99	0.98	0.98
$(NH_3)_1 \cdot (TFA)_1 \cdot (H_2O)_1$	0.00	0.01	0.01	0.02	0.02

$(NH_3)_1 \cdot (TFA)_1 \cdot (H_2O)_2$	0.00	0.00	0.00	0.00	0.00
$(SA)_1 \cdot (NH_3)_1$	0.30	0.09	0.04	0.02	0.01
$(SA)_1 \cdot (NH_3)_1 \cdot (H_2O)_1$	0.00	0.00	0.00	0.00	0.00
$(SA)_1 \cdot (NH_3)_1 \cdot (H_2O)_2$	0.68	0.84	0.86	0.84	0.82
$(SA)_1 \cdot (NH_3)_1 \cdot (H_2O)_3$	0.03	0.07	0.10	0.14	0.16
$(SA)_1 \cdot (NH_3)_1 \cdot (TFA)_1$	0.05	0.03	0.02	0.01	0.01
$(SA)_1 \cdot (NH_3)_1 \cdot (TFA)_1 \cdot (H_2O)_1$	0.91	0.90	0.86	0.82	0.77
$(SA)_1 \cdot (NH_3)_1 \cdot (TFA)_1 \cdot (H_2O)_2$	0.04	0.07	0.10	0.13	0.16
$(SA)_1 \cdot (NH_3)_1 \cdot (TFA)_1 \cdot (H_2O)_3$	0.00	0.01	0.02	0.04	0.06
$(SA)_1 \cdot (NH_3)_2 \cdot (TFA)_1$	0.31	0.12	0.05	0.03	0.02
$(SA)_1 \cdot (NH_3)_2 \cdot (TFA)_1 \cdot (H_2O)_1$	0.42	0.32	0.22	0.15	0.11
$(SA)_1 \cdot (NH_3)_2 \cdot (TFA)_1 \cdot (H_2O)_2$	0.17	0.27	0.27	0.25	0.23
$(SA)_1 \cdot (NH_3)_2 \cdot (TFA)_1 \cdot (H_2O)_3$	0.10	0.29	0.46	0.57	0.64
			220 K		
SA	0.63	0.40	0.26	0.18	0.13
$(SA)_1 \cdot (H_2O)_1$	0.27	0.34	0.34	0.32	0.29
$(SA)_1 \cdot (H_2O)_2$	0.10	0.25	0.38	0.47	0.54
$(SA)_1 \cdot (H_2O)_3$	0.00	0.01	0.02	0.03	0.04
TFA	0.90	0.82	0.74	0.67	0.61
$(TFA)_1 \cdot (H_2O)_1$	0.09	0.17	0.23	0.28	0.31
$(TFA)_1 \cdot (H_2O)_2$	0.00	0.02	0.03	0.05	0.07
$(SA)_1 \cdot (TFA)_1$	0.58	0.36	0.24	0.17	0.12
$(SA)_1 \cdot (TFA)_1 \cdot (H_2O)_1$	0.32	0.40	0.40	0.37	0.34
$(SA)_1 \cdot (TFA)_1 \cdot (H_2O)_2$	0.10	0.25	0.37	0.46	0.53
$(SA)_1 \cdot (TFA)_1 \cdot (H_2O)_3$	0.00	0.00	0.00	0.01	0.01
NH_3	1.00	1.00	1.00	1.00	1.00
$(NH_3)_1 \cdot (H_2O)_2$	0.00	0.00	0.00	0.00	0.00
$(NH_3)_1 \cdot (H_2O)_2$	0.00	0.00	0.00	0.00	0.00
$(NH_3)_1 \cdot (TFA)_1$	1.00	0.99	0.99	0.98	0.98
$(NH_3)_1 \cdot (TFA)_1 \cdot (H_2O)_1$	0.00	0.01	0.01	0.02	0.02
$(NH_3)_1 \cdot (TFA)_1 \cdot (H_2O)_2$	0.00	0.00	0.00	0.00	0.00
$(SA)_1 \cdot (NH_3)_1$	0.23	0.07	0.03	0.02	0.01
$(SA)_1 \cdot (NH_3)_1 \cdot (H_2O)_1$	0.00	0.00	0.00	0.00	0.00
$(SA)_1 \cdot (NH_3)_1 \cdot (H_2O)_2$	0.74	0.87	0.87	0.85	0.83
$(SA)_1 \cdot (NH_3)_1 \cdot (H_2O)_3$	0.03	0.07	0.10	0.13	0.16
$(SA)_1 \cdot (NH_3)_1 \cdot (TFA)_1$	0.04	0.02	0.01	0.01	0.01
$(SA)_1 \cdot (NH_3)_1 \cdot (TFA)_1 \cdot (H_2O)_1$	0.92	0.90	0.86	0.82	0.77
$(SA)_1 \cdot (NH_3)_1 \cdot (TFA)_1 \cdot (H_2O)_2$	0.04	0.07	0.10	0.13	0.16
$(SA)_1 \cdot (NH_3)_1 \cdot (TFA)_1 \cdot (H_2O)_3$	0.00	0.01	0.03	0.04	0.06
$(SA)_1 \cdot (NH_3)_2 \cdot (TFA)_1$	0.23	0.08	0.04	0.02	0.01
$(SA)_1 \cdot (NH_3)_2 \cdot (TFA)_1 \cdot (H_2O)_1$	0.44	0.30	0.20	0.13	0.10
$(SA)_1 \cdot (NH_3)_2 \cdot (TFA)_1 \cdot (H_2O)_2$	0.21	0.29	0.28	0.26	0.23
$(SA)_1 \cdot (NH_3)_2 \cdot (TFA)_1 \cdot (H_2O)_3$	0.12	0.33	0.48	0.59	0.66

Table S11. Ratios ($\beta C/\Sigma\gamma$) between monomer molecule collisions and evaporation coefficients of $(SA)_1\cdot(NH_3)_{1\text{-}2}\cdot(TFA)_1$ cluster at different relative humidities (RHs) and different temperatures. $C = 1.0\times10^6$ molecules cm^{-3}.

Clusters	$\beta C/\Sigma\gamma$				
	RH=20%	RH=40%	RH=60%	RH=80%	RH=100%
			240 K		
$(SA)_1\cdot(TFA)_1$	9.60×10^{-6}	8.04×10^{-6}	6.91×10^{-6}	6.09×10^{-6}	5.46×10^{-6}
$(NH_3)_1\cdot(TFA)_1$	1.29×10^{-8}	1.19×10^{-8}	1.09×10^{-8}	1.00×10^{-8}	9.19×10^{-9}
$(SA)_1\cdot(NH_3)_1\cdot(TFA)_1$	2.02×10^{-4}	1.60×10^{-4}	1.07×10^{-4}	7.89×10^{-5}	9.19×10^{-6}
$(SA)_1\cdot(NH_3)_2\cdot(TFA)_1$	1.39×10^{-5}	1.52×10^{-5}	1.99×10^{-5}	2.62×10^{-5}	3.35×10^{-5}
			230 K		
$(SA)_1\cdot(TFA)_1$	4.71×10^{-5}	3.99×10^{-5}	3.47×10^{-5}	3.09×10^{-5}	2.79×10^{-5}
$(NH_3)_1\cdot(TFA)_1$	4.33×10^{-8}	3.98×10^{-8}	3.66×10^{-8}	3.36×10^{-8}	3.09×10^{-8}
$(SA)_1\cdot(NH_3)_1\cdot(TFA)_1$	1.34×10^{-3}	9.60×10^{-4}	6.35×10^{-4}	1.19×10^{-5}	3.65×10^{-4}
$(SA)_1\cdot(NH_3)_2\cdot(TFA)_1$	7.08×10^{-5}	8.54×10^{-5}	1.18×10^{-4}	1.59×10^{-4}	2.08×10^{-4}
			220 K		
$(SA)_1\cdot(TFA)_1$	2.70×10^{-4}	2.70×10^{-4}	2.49×10^{-4}	2.29×10^{-4}	2.12×10^{-4}
$(NH_3)_1\cdot(TFA)_1$	1.66×10^{-7}	1.53×10^{-7}	1.41×10^{-7}	1.30×10^{-7}	1.19×10^{-7}
$(SA)_1\cdot(NH_3)_1\cdot(TFA)_1$	1.02×10^{-2}	6.42×10^{-3}	4.21×10^{-3}	3.09×10^{-3}	2.42×10^{-3}
$(SA)_1\cdot(NH_3)_2\cdot(TFA)_1$	4.37×10^{-4}	5.88×10^{-4}	8.51×10^{-4}	1.18×10^{-3}	1.55×10^{-3}

Table S12. Gibbs free formation energies (ΔG, kcal mol^{-1}) of the studied clusters at different pressures at the RI-CC2/aug-cc-pV(T + d)Z//M06-2X/6-311++G(3df,3pd) level of theory.

Clusters	ΔG (kcal mol^{-1})			
	p = 0.2 atm	p = 0.4 atm	p = 0.6 atm	p = 0.8 atm
$(TFA)_2$	-6.17	-6.50	-6.69	-6.83
$(TFA)_3$	-5.17	-5.83	-6.22	-6.49
$(SA)_1 \cdot (TFA)_1$	-8.47	-8.80	-8.99	-9.13
$(SA)_1 \cdot (TFA)_2$	-15.04	-15.71	-16.09	-16.37
$(SA)_2 \cdot (TFA)_1$	-16.32	-16.98	-17.37	-17.64
$(SA)_2$	-9.63	-9.96	-10.15	-10.29
$(SA)_3$	-16.88	-17.54	-17.92	-18.20
$(SA)_2 \cdot (NH_3)_1$	-25.69	-26.35	-26.74	-27.01
$(SA)_2 \cdot (NH_3)_2$	-36.73	-37.72	-38.30	-38.71
$(SA)_3 \cdot (NH_3)_1$	-37.57	-38.56	-39.14	-39.55
$(SA)_3 \cdot (NH_3)_2$	-54.03	-55.35	-56.12	-56.67
$(SA)_3 \cdot (NH_3)_3$	-68.73	-70.38	-71.35	-72.03
$(SA)_1 \cdot (NH_3)_1$	-8.35	-8.68	-8.88	-9.01
$(SA)_1 \cdot (NH_3)_1 \cdot (TFA)_1$	-17.73	-18.39	-18.78	-19.05
$(SA)_1 \cdot (NH_3)_2 \cdot (TFA)_1$	-27.42	-28.41	-28.99	-29.40
$(SA)_1 \cdot (NH_3)_1 \cdot (TFA)_2$	-26.45	-27.45	-28.03	-28.44
$(SA)_1 \cdot (NH_3)_2 \cdot (TFA)_2$	-36.16	-37.49	-38.26	-38.81
$(SA)_1 \cdot (NH_3)_3 \cdot (TFA)_2$	-42.89	-44.54	-45.51	-46.20
$(NH_3)_1 \cdot (TFA)_1$	-5.49	-5.82	-6.01	-6.15
$(SA)_2 \cdot (NH_3)_1 \cdot (TFA)_1$	-34.14	-35.13	-35.71	-36.12
$(SA)_2 \cdot (NH_3)_2 \cdot (TFA)_1$	-44.90	-46.23	-47.00	-47.55
$(SA)_2 \cdot (NH_3)_3 \cdot (TFA)_1$	-59.30	-60.96	-61.92	-62.61
$(NH_3)_1 \cdot (TFA)_2$	-11.22	-11.89	-12.27	-12.55
$(NH_3)_2 \cdot (TFA)_2$	-16.02	-17.01	-17.59	-18.00
$(NH_3)_1 \cdot (TFA)_3$	-17.47	-18.46	-19.04	-19.45
$(NH_3)_2 \cdot (TFA)_3$	-30.40	-31.73	-32.50	-33.05
$(NH_3)_3 \cdot (TFA)_3$	-36.90	-38.56	-39.52	-40.21

Table S13. Particle formation rates (J, cm^{-3} s^{-1}) of the studied clusters at different pressures at 240 K. [SA] = 5.0×10^6 molecules cm^{-3}, [NH_3] = 1.0×10^{11} molecules cm^{-3}, [TFA] = 1.0×10^6–1.0×10^8 molecules cm^{-3}.

[TFA]	J (cm^{-3} s^{-1})				
	p = 0.2 atm	p = 0.4 atm	p = 0.6 atm	p = 0.8 atm	p = 1.0 atm
1.0×10^6	18.68	18.69	18.74	18.68	18.70
2.0×10^6	21.99	22.00	22.06	22.00	22.02
3.0×10^6	25.20	25.23	25.29	25.22	25.23
4.0×10^6	28.33	28.36	28.43	28.35	28.36
5.0×10^6	31.36	31.41	31.48	31.39	31.40
6.0×10^6	34.32	34.37	34.44	34.35	34.36
7.0×10^6	37.20	37.25	37.33	37.23	37.24
8.0×10^6	40.00	40.06	40.14	40.04	40.05
9.0×10^6	42.73	42.80	42.88	42.77	42.78
1.0×10^7	45.38	45.46	45.55	45.44	45.44
2.0×10^7	68.67	68.79	68.91	68.76	68.75
3.0×10^7	87.29	87.44	87.58	87.39	87.39
4.0×10^7	102.59	102.76	102.92	102.70	102.69
5.0×10^7	115.46	115.63	115.81	115.56	115.56
6.0×10^7	126.49	126.67	126.85	126.59	126.59
7.0×10^7	136.11	136.28	136.48	136.19	136.21
8.0×10^7	144.63	144.79	144.99	144.69	144.71
9.0×10^7	152.26	152.41	152.62	152.30	152.33
1.0×10^8	159.18	159.32	159.53	159.20	159.24

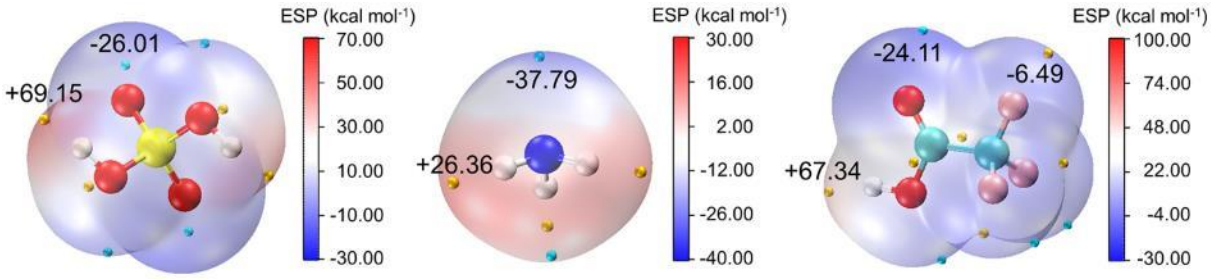

Fig. S1. The electrostatic potential (ESP, kcal mol^{-1}) mapped molecular van der Walls (vdW) surfaces of the SA, NH_3, and TFA molecules at the M06-2X/6-311++G(3df,3pd) level of theory. Surface local minima and maxima of the ESP are shown as yellow and cyan dots, respectively. The C, H, N, O, S, and F atoms are shown as cyan, white, blue, red, yellow, and pink spheres, respectively.

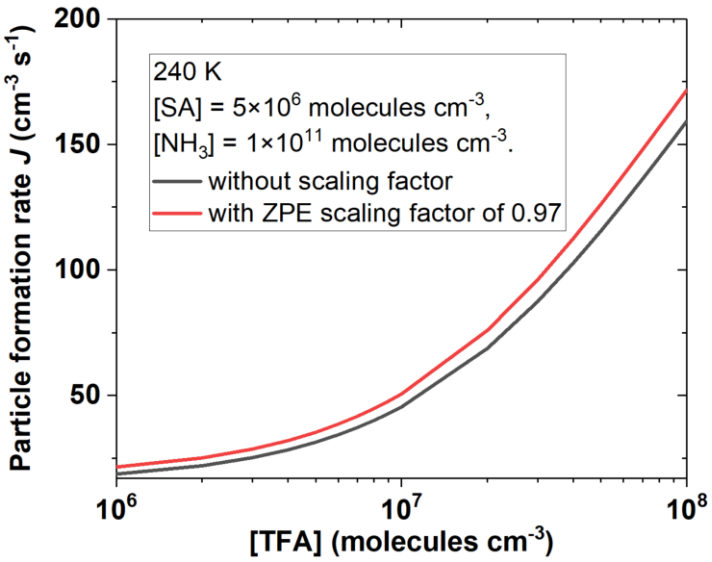

Fig. S2. Particle formation rates (J, cm^{-3} s^{-1}) at different [TFA] and 240 K. [SA] = 5.0×10^6 molecules cm^{-3}, [NH_3] = 1.0×10^{11} molecules cm^{-3}. The black and red lines correspond to the simulated J based on the calculated Gibbs free energy of cluster formation without scaling factor and with Zero Point Energy (ZPE) scaling factor of 0.97.

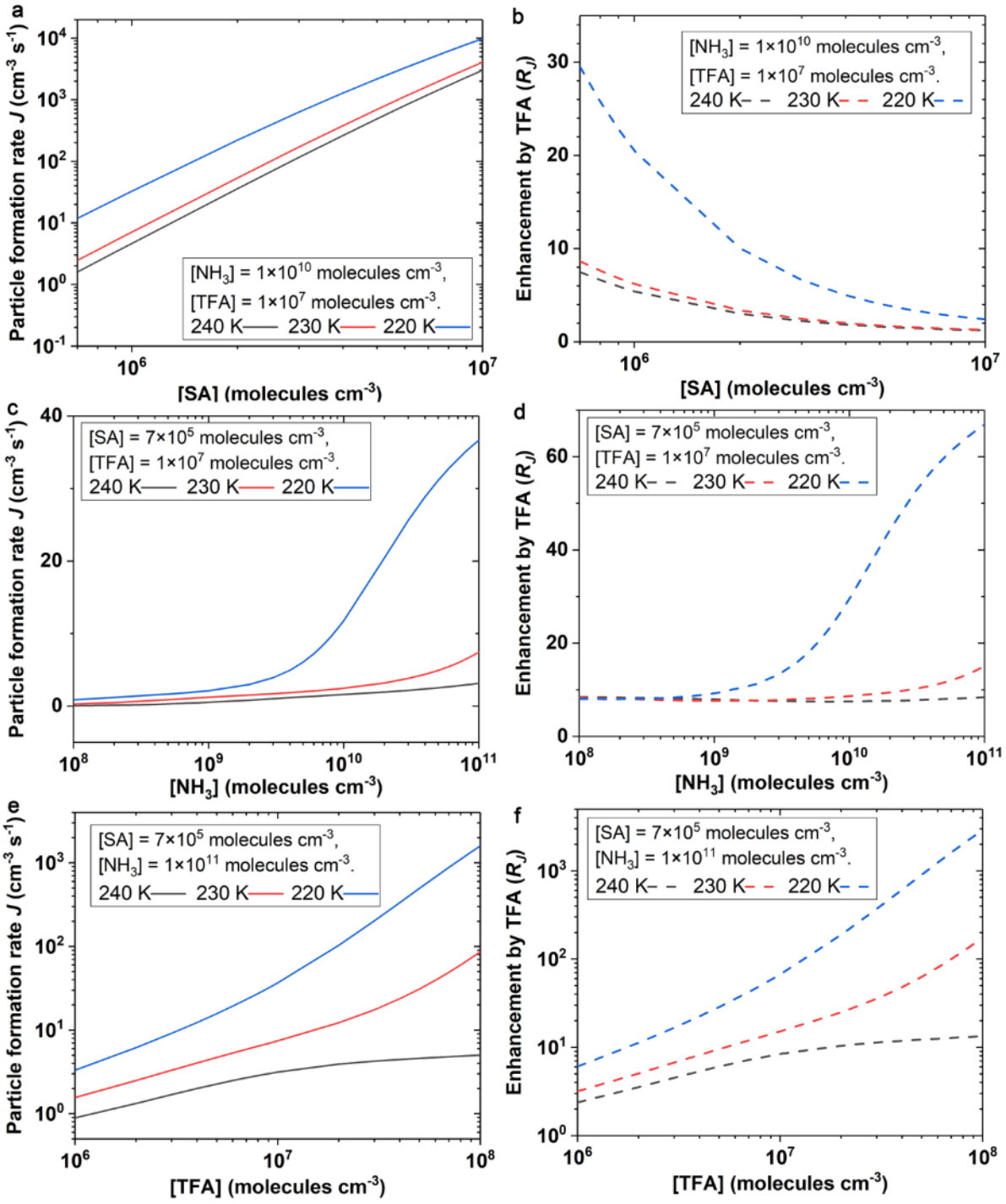

Fig. S3. Particle formation rates (J, cm^{-3} s^{-1}) at different temperatures as a function of (a) [SA], (c) [NH_3], and (e) [TFA]. Enhancement on particle formation rate by TFA (R_J, $R_J = J_{SA\text{-}NH_3\text{-}TFA}/J_{SA\text{-}NH_3}$) at different temperatures as a function of (b) [SA], (d) [NH_3], and (f) [TFA]. Black, red, and blue lines are corresponding to the J at 240 K, 230 K, and 220 K, respectively. CS = 2.0×10^{-3} s^{-1}.

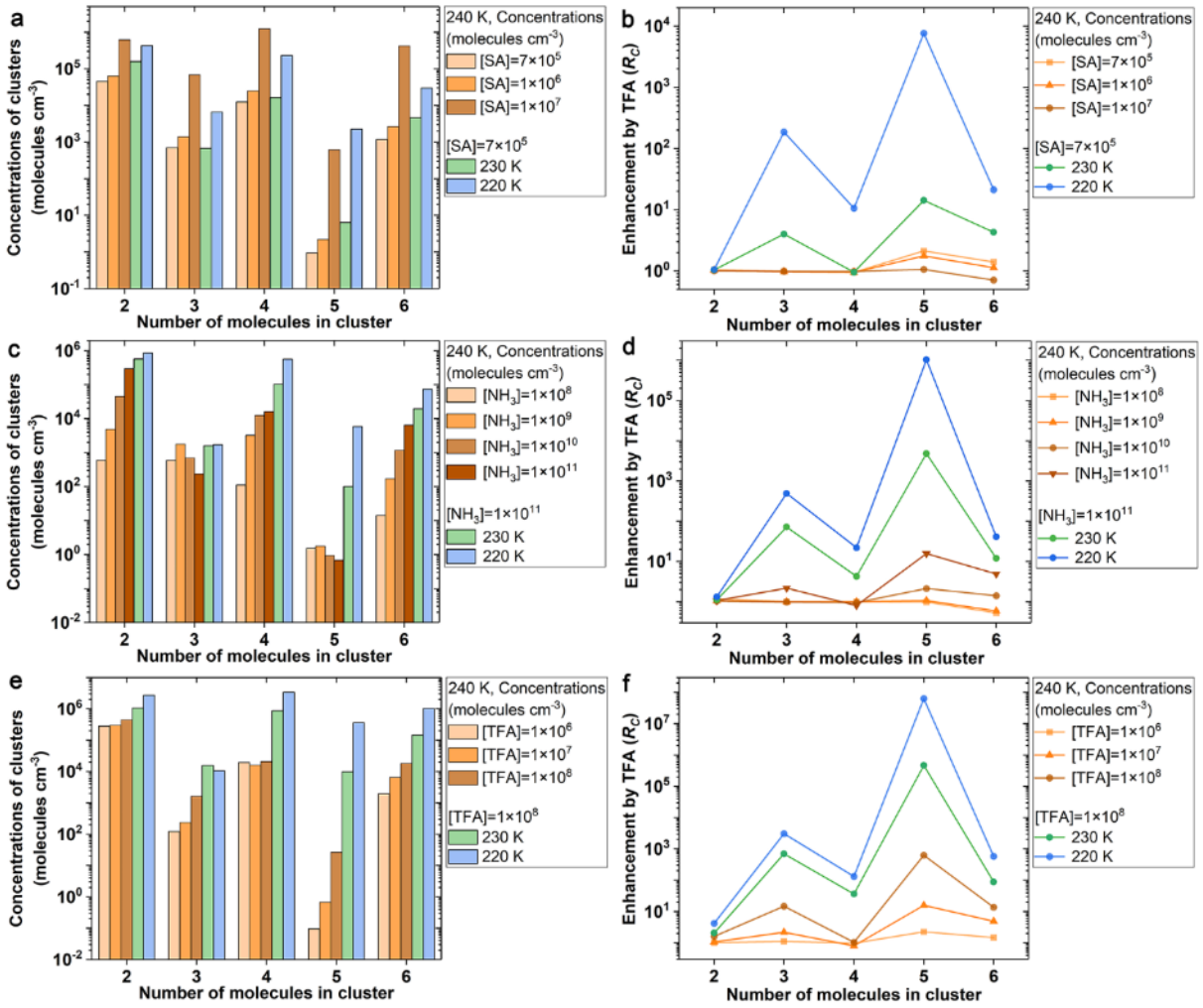

Fig. S4. Concentrations (molecules cm^{-3}) at different temperatures as a function of (a) [SA], (c) [NH_3], and (e) [TFA]. Enhancement by TFA on concentrations of clusters (R_C, $R_C = C_{SA\text{-}NH_3\text{-}TFA}/C_{SA\text{-}NH_3}$) at different temperatures as a function of (b) [SA], (d) [NH_3], and (f) [TFA]. CS = 2.0×10^{-3} s^{-1}. (a) and (b): [NH_3] = 1.0×10^{10} molecules cm^{-3}, [TFA] = 1.0×10^{7} molecules cm^{-3}. (c) and (d): [SA] = 7.0×10^{5} molecules cm^{-3}, [TFA] = 1.0×10^{7} molecules cm^{-3}. (e) and (f): [SA] = 7.0×10^{5} molecules cm^{-3}, [NH_3] = 1.0×10^{11} molecules cm^{-3}.

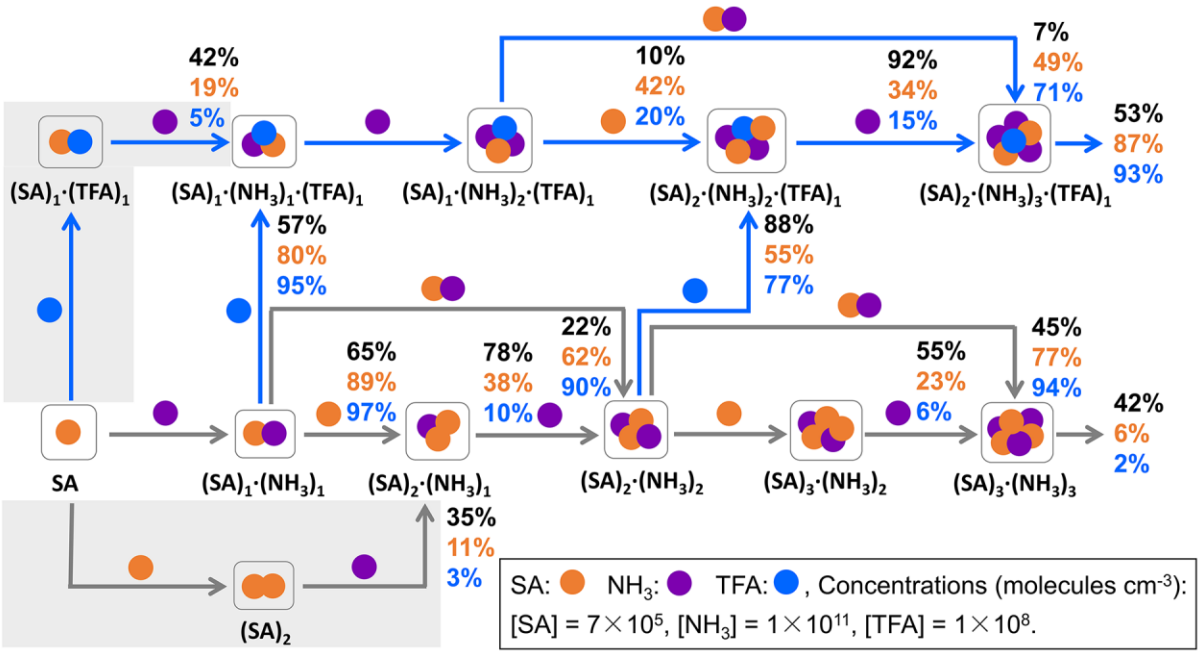

Fig. S5. Main cluster formation pathways of SA-NH_3-TFA clusters at [SA] = 7×10^5 molecules cm^{-3}, [NH_3] = 1×10^{11} molecules cm^{-3}, and [TFA] = 1×10^8 molecules cm^{-3}. Blue arrows show the pathways involving TFA and grey arrows show the pathways without TFA. The pathways covered by the light grey shadow are only present at 240 K and 230 K, but not present at 220 K. The pathways without light grey shadow are the common pathways at different temperatures (240 K, 230 K, and 220 K). The values of contribution (percentage) shown in black, orange, and blue are corresponding to the contributions to the formation of the relevant larger clusters at 240 K, 230 K, and 220 K.

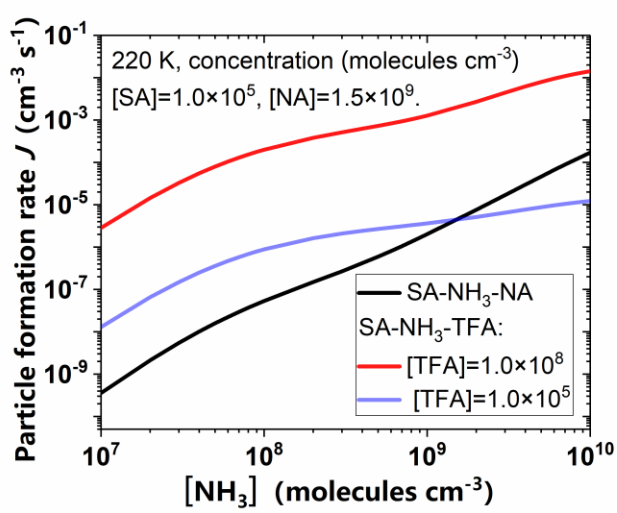

Fig. S6. Comparison of particle formation rates (J, cm^{-3} s^{-1}) between SA–NH_3–TFA and SA–NH_3–NA under selected upper tropospheric sensitivity conditions as a function of [NH_3] at 220 K. Blue and red lines show the J for SA–NH_3–TFA at the concentration of TFA at 1.0×10^8 molecules cm^{-3} and 1.0×10^5 molecules cm^{-3}, respectively. Black line shows the J for SA–NH_3–NA. [SA] = 1.0×10^5 molecules cm^{-3}, [NA] = 1.5×10^9 molecules cm^{-3}.

References

[1] Y. Lu, L. Liu, A. Ning, et al., Atmospheric sulfuric acid-dimethylamine nucleation enhanced by trifluoroacetic acid, Geophys. Res. Lett. 47 (2) (2020) e2019GL085627.

[2] L. Liu, F. Yu, L. Du, et al., Rapid sulfuric acid-dimethylamine nucleation enhanced by nitric acid in polluted regions, Proc. Natl. Acad. Sci. U. S. A. 118 (35) (2021) e2108384118.

[3] L. Yao, O. Garmash, F. Bianchi, et al., Atmospheric new particle formation from sulfuric acid and amines in a chinese megacity, Science 361 (6399) (2018) 278–281.

[4] J. Almeida, S. Schobesberger, A. Kürten, et al., Molecular understanding of sulphuric acid-amine particle nucleation in the atmosphere, Nature 502 (7471) (2013) 359–363.

[5] A. Kürten, C. Li, F. Bianchi, et al., New particle formation in the sulfuric acid-dimethylamine-water system: reevaluation of cloud chamber measurements and comparison to an aerosol nucleation and growth model, Atmos. Chem. Phys. 18 (2) (2018) 845–863.

[6] C. Riplinger and F. Neese, An efficient and near linear scaling pair natural orbital based local coupled cluster method, J. Chem. Phys. 138 (3) (2013)

[7] C. Riplinger, B. Sandhoefer, A. Hansen, et al., Natural triple excitations in local coupled cluster calculations with pair natural orbitals, J. Chem. Phys. 139 (13) (2013)

[8] J. Dunning, K. A. Peterson, and A. K. Wilson, Gaussian basis sets for use in correlated molecular calculations. X. The atoms aluminum through argon revisited, J. Chem. Phys. 114 (21) (2001) 9244–9253.

[9] M. J. McGrath, T. Olenius, I. K. Ortega, et al., Atmospheric cluster dynamics code: a flexible method for solution of the birth-death equations, Atmos. Chem. Phys. 12 (5) (2012) 2345–2355.

[10] S. Jiang, Y.-R. Liu, T. Huang, et al., Towards fully ab initio simulation of atmospheric aerosol nucleation, Nat. Commun. 13 (1) (2022) 6067.

[11] J. Almeida, S. Schobesberger, A. Kürten, et al., Molecular understanding of sulphuric acid-amine particle nucleation in the atmosphere, Nature 502 (7471) (2013) 359–363.

[12] S. Chapman and T. G. Cowling, *The Mathematical Theory of Non-Uniform Gases*. University Press: Cambridge, U.K. (1970) .

[13] T. Lu and F. Chen, Multiwfn: a multifunctional wavefunction analyzer, J. Comput. Chem. 33 (5) (2012) 580–592.

[14] M. J. McGrath, T. Olenius, I. K. Ortega, et al., Atmospheric cluster dynamics code: a flexible method for solution of the birth-death equations, Atmos. Chem. Phys. 12 (5) (2012) 2345–2355.

[15] B. Zhang, Z. Zhai, and J. Zhang, Distribution of trifluoroacetic acid in gas and particulate phases in Beijing from 2013 to 2016, Sci. Total Environ. 634 (2018) 471–477.

[16] J. Wu, J. W. Martin, Z. Zhai, et al., Airborne trifluoroacetic acid and its fraction from the degradation of HFC-134a in Beijing, China, Environ. Sci. Technol. 48 (7) (2014) 3675–3681.

[17] A. Breuninger, P. Joppe, J. Wilsch, et al., Organic aerosols mixing across the tropopause and its implication for anthropogenic pollution of the UTLS, Atmos. Chem. Phys. 25 (22) (2025) 16533–16551.

[18] R. Dodangodage, P. F. Bernath, C. Boone, et al., The first satellite measurements of HFC-125 by the ACE-FTS: long-term trends and distribution in the Earth's upper troposphere and lower stratosphere, J. Quant. Spectrosc. Radiat. Transf. 330 (July 2024) (2025) 109218.

[19] J. L. Bao, X. Zhang, and D. G. Truhlar, Predicting pressure-dependent unimolecular rate constants using variational transition state theory with multidimensional tunneling combined with system-specific quantum RRK theory: a definitive test for fluoroform dissociation, Phys. Chem. Chem. Phys. 18 (25) (2016) 16659–16670.